

8-2017

A Cross-Layer Design for Reducing Packet Loss Caused by Fading in a Mobile Ad Hoc Network

William Derek Johnson
Clemson University

Follow this and additional works at: https://tigerprints.clemson.edu/all_theses

Recommended Citation

Johnson, William Derek, "A Cross-Layer Design for Reducing Packet Loss Caused by Fading in a Mobile Ad Hoc Network" (2017). *All Theses*. 2755.

https://tigerprints.clemson.edu/all_theses/2755

This Thesis is brought to you for free and open access by the Theses at TigerPrints. It has been accepted for inclusion in All Theses by an authorized administrator of TigerPrints. For more information, please contact kokeefe@clemson.edu.

A CROSS-LAYER DESIGN FOR REDUCING PACKET LOSS CAUSED BY FADING IN A MOBILE AD HOC NETWORK

A Thesis
Presented to
the Graduate School of
Clemson University

In Partial Fulfillment
of the Requirements for the Degree
Master of Science
Computer Engineering

by
William Derek Johnson
August 2017

Accepted by:
Dr. Harlan Russell, Committee Chair
Dr. Kuang-Ching Wang
Dr. Yongqiang Wang

Abstract

We investigate methods for reducing packet loss in mobile ad hoc networks (MANETs) caused by the presence of fading. The modeled system employs an adaptive transmission protocol. This protocol works well when link performance is consistent and predictable, but system performance deteriorates when link quality begins to vary. A log-normal block fading model is implemented to test system performance with time-varying link performance. We propose two different methods for addressing the effects of fading. First we propose the transmission success probability (TSP) link-rate control protocol, which uses link performance measures to modify the existing adaptive transmission protocol and reduce the number of packets lost due to fading. Secondly we show that modifying the routing metric can improve system performance. We show that a cross-layer design for the TSP protocols and routing metrics that jointly considers both link and network performance results in better system performance compared to selecting each protocol separately.

Table of Contents

	Page
Title Page	i
Abstract	ii
List of Tables	v
List of Figures	vi
1 Introduction	1
2 Related Work	4
3 System Design	7
3.1 Channel Model	7
3.2 Neighbors	8
3.3 Lyui’s Algorithm	9
3.4 Adaptive Transmission	11
4 Methods for Handling Variable Fading Effects	12
4.1 Fading Model	12
4.2 Transmission Success Probability Link Rate Control	13
4.3 Routing Metrics	15
5 Simulation Details	19
5.1 Initialization of Network	19
5.2 Traffic Generation and Routing	21
5.3 Network Performance Measures	22
6 Results	24
6.1 Performance of TSP Link Rate Control	26
6.2 Importance of Investigating the Routing Metric With the TSP Protocol	30
6.3 Impact of the TSP Protocol Threshold	37
6.4 Performance Without the Adaptive Transmission Rate Protocol	40
6.5 System Performance in Different Network Environments	44
7 Conclusions	52

Table of Contents Continued

	Page
References	54

List of Tables

Table	Page
3.1 Candidate slot numbers based on color number	9
3.2 Spreading factors used for different mean SNIR estimates	11
6.1 Unchanged network parameters	25
6.2 Default parameters that may be changed	25
6.3 Network density measures based on field length	44

List of Figures

Figure	Page
4.1 Transmission Success Probability link rate control pseudo-code	14
6.1 Percent Dropped vs. Arrival Rate for: No Fading, SNIR, SNIR.ETX, SNIR + TSP, and SNIR.ETX + TSP	27
6.2 Throughput vs. Arrival Rate for: No Fading, SNIR, SNIR + TSP, SNIR.ETX, and SNIR.ETX + TSP	29
6.3 End-to-End Delay vs. Arrival Rate for: No Fading, SNIR, SNIR + TSP, SNIR.ETX, and SNIR.ETX + TSP	30
6.4 Percent Dropped vs. Arrival Rate for: Min Hop, Min Hop + TSP, ETX, ETX + TSP, and SNIR.ETX + TSP	31
6.5 Percent Dropped vs. Arrival Rate for: SNIR.ETX + TSP, SNIR.StdDev, and SNIR.StdDev + TSP	32
6.6 Break down of dropped packets for: No Fading, SNIR, SNIR + TSP, SNIR.ETX, and SNIR.ETX + TSP	34
6.7 Break down of dropped packets for: SNIR.ETX, SNIR.ETX + TSP, SNIR.StdDev, and SNIR.StdDev + TSP	35
6.8 Break down of dropped packets for: SNIR.ETX, SNIR.ETX + TSP, ETX, and ETX + TSP	36
6.9 Threshold comparison of percent dropped vs. arrival rate for: TSP threshold values {0.4, 0.5, 0.6, 0.7, 0.8, 0.9}	38
6.10 Threshold comparison of network throughput vs. arrival rate for: TSP threshold values {0.4, 0.5, 0.6, 0.7, 0.8, 0.9}	39
6.11 Threshold comparison of end-to-end delay vs. arrival rate for: TSP threshold values {0.4, 0.5, 0.6, 0.7, 0.8, 0.9}	40
6.12 Percent Dropped vs. Arrival Rate without adaptive transmission for: No Fading, SNIR, SNIR.ETX, SNIR.StdDev, Min Hop, and ETX	41
6.13 Network Throughput vs. Arrival Rate without adaptive transmission for: No Fading, SNIR, SNIR.ETX, SNIR.StdDev, Min Hop, and ETX	42
6.14 End-to-End Delay vs. Arrival Rate without adaptive transmission for: No Fading, SNIR, SNIR.ETX, SNIR.StdDev, Min Hop, and ETX	43
6.15 Percent Dropped vs. Arrival Rate with field lengths of 1500 and 1250 m for: No Fading, SNIR, SNIR + TSP, SNIR.ETX, and SNIR.ETX + TSP	46
6.16 Re-Transmission Drops vs. Arrival Rate with field lengths of 1500m and 1250m for: SNIR and SNIR.ETX	47

List of Figures Continued

Figure	Page
6.17 End-to-End Delay vs. Arrival rate with field lengths of 1500m and 1250m for: No Fading, SNIR, SNIR + TSP, SNIR.ETX, and SNIR.ETX + TSP	48
6.18 Percent Dropped vs. Arrival Rate with 0-7dB and 0-10dB of fading for: No Fading, SNIR, SNIR + TSP, SNIR.ETX, and SNIR.ETX + TSP	50
6.19 Percent Dropped vs. Arrival Rate with 0-3dB of fading for: No Fading, SNIR, SNIR + TSP, SNIR.ETX, and SNIR.ETX + TSP	51

Chapter 1

Introduction

A mobile ad hoc network, or MANET, is a wireless network that consists of mobile radio nodes. Each node in the network helps to forward traffic from source to destination, usually over multiple hops. This requires each node in the network to make routing decisions when forwarding packets. An advantage of MANET is the ability to operate when there is no infrastructure present. Quickly forming a network utilizing just the nodes makes them an attractive technology for military and disaster response operations.

Whenever multiple nodes use the same transmission medium, a media access control (MAC) protocol must be used to allocate the available channel resources. There are two main types of MAC protocols, contention and non-contention based. In contention based MAC protocols, such as ALOHA and CSMA, nodes compete for use of the channel and are awarded access on a first-come first-served basis. The contention in these protocols can result in the collision of packet transmissions which degrades network performance when there is a heavy load on the system. Non-contention based MAC protocols avoid collisions in the network, making them better suited for heavily loaded systems but result in wasted channel resources when there is not as much traffic. Two of the most common non-contention based protocols are time-division multiple access (TDMA) and frequency-division multiple access (FDMA). As the names suggest these protocols avoid transmission collisions by dividing the channel resources of either time or frequency. These channel

resources are then pre-allocated to individual nodes to use when needed. In this thesis we focus on a TDMA based system that improves channel utilization by allowing multiple nodes to transmit at the same time if they are far enough apart.

Even in a collision-free environment, a combination of factors such as multiple-access interference (MAI) and channel noise can result in a packet not being received successfully. This makes it important to model links based on the signal-to-noise-plus-interference-ratio (SNIR) experienced during a transmission between two nodes. Using a simple graph model for links can yield an optimistic view of network performance which may not translate well to real world operation.

In addition to MAI and channel noise, fading also affects the ability of nodes to receive transmissions. There are many different models for fading. These models are broken down into two categories, fast fading and slow fading. In fast fading models the channel can cause changes in signal amplitude and phase multiple times within a single transmission. Slow fading models result in a slower change in signal properties and there is usually no change within a transmission. Popular models for fading include, Rayleigh fading, Rician fading, and log-normal fading. These models cause variability in the measured SNIR for transmissions over a link. This variability can make the performance of certain links unpredictable and can reduce the overall performance in the network. In this thesis we use a block fading model which holds the fading effect of a link constant throughout a time slot.

Many radio systems have the ability to adapt properties of the transmission. This allows the system to dynamically respond to the changing physical environment. The system may transmit at a faster data rate or lower power to take advantage of a better link quality. The adaptive transmission protocol should respond quickly to the changing link quality to ensure the best system performance.

When simulating and designing protocols for wireless networks, it is important to accurately model the physical environment. Using estimated SNIR measures provides a more accurate model than a simple graph-based approach, but it is also important to take into account the effects of fading. In this thesis we show that the presence of fading

significantly decreases network performance, and we propose two methods for mitigating the impacts of fading. First, we show that adjusting the adaptive transmission protocol to take link variability into account significantly improves network performance when fading is present. Second, we show that modifying how packets are routed can offer limited success in addressing the issues presented by a fading environment. We show that a cross-layer design for the adaptive transmission and routing protocols that jointly considers both link and network performance results in better system performance compared to selecting each protocol separately.

Chapter 2

Related Work

Routing is key to the performance of any multi-hop packet network, and there has been a lot of research in routing for use in MANETs. The authors in [1] and [2] list several popular methods for exchanging routing information in a MANET. While the routing protocol itself is very important to the performance of the network, we focus on how to weight the cost of links in the route. The min hop count routing metric is well known and widely used because of its ease of implementation, but many metrics provide better network performance. In [3] a routing metric is proposed that works with an adaptive transmission protocol to reduce the energy used to transmit a packet. The authors show how cross-layer information can be used to improve the routing metric. The author in [4] also uses a cross-layer approach to routing. The link weights include parameters from the physical and MAC layers. The expected transmission count (ETX) routing metric, first described in [5], describes a metric that can improve network throughput by reducing the total number of transmissions required to deliver a packet from source to destination. This is achieved by keeping a running count of the packet error probability of a link.

The characteristics of MANETs make channel access challenging, which has resulted in a lot of research in the area. Several channel access protocols for MANETs are described in [6], but the article focuses on contention-based MAC. An example of a TDMA scheme that is used for an operational MANET is described in [7] and [8]. Lyui's algorithm described in

[9] uses a network coloring to assign slots to nodes in a way that allows multiple nodes to transmit in the same slot while still keeping transmissions collision free. Lyui's algorithm is further described in [10] and the authors also provide a method to quickly solve scheduling conflicts caused by mobility. While a graph-based simulation is used in [10] to show the performance of Lyui's algorithm, the investigations in [4] show that the scheduling algorithm still works well when noise and multiple-access interference are accounted for. The authors in [11] propose a scheduling algorithm that can result in lower end-to-end delay than Lyui's algorithm in some scenarios. Even with an efficient scheduling of nodes, TDMA schemes still suffer when the system load is light. However, the authors in [12] provide a method for recovering scheduled time slots that are not being used. This results in fewer unused slots and better network performance.

The ability to adapt transmissions to the link conditions can improve overall network performance. An adaptive transmission protocol described in [13] uses error counts from the decoder to detect link quality. This protocol can be used to reduce the energy needed for transmissions. One instance where adaptive transmission has captured a lot of attention is the IEEE 802.11 standard. This standard already includes different supported transmission rates, but does not describe a method for quickly adapting the rate. In [14] received signal strength estimates are used to determine link qualities and adjust the transmission rate. A protocol that adapts the rate based on successful and unsuccessful transmissions is described in [15]. In this protocol the transmission rate increases for successful transmissions and decreases for failures.

Rappaport explains how to model the physical channel of wireless communications systems in [16]. This text provides an understanding of important factors to model in simulation but focuses primarily on fast fading models. An example of a block fading model is implemented using Markov chains in [17] and [18]. In this model the fading environment is assumed to be constant during the duration of a transmission, and the analysis shows that this assumption still results in an accurate model. The log-normal fading model is popular for modeling slow varying fading environments. A recent study in [19] shows interest in

using the log-normal fading model for future millimeter wave systems. In [20] a Markov chain is used to model several different fading environments, including log-normal fading, and [21] shows a framework for simulating the log-normal model. While there is a lot of work on fading models, most focus on bit error probabilities. In this thesis we are interested in packet error probabilities, so we will focus on how fading impacts the SNIR instead of individual bits.

Chapter 3

System Design

In this chapter we describe the details of how the system operates and describe the physical channel model. We discuss how neighborhoods are formed and give an overview of Lyui's algorithm for transmission scheduling. We also describe how the adaptive transmission protocol works.

3.1 Channel Model

The channel model used is taken from [4] and the references therein. Nodes in the network communicate using direct-sequence spread-spectrum (DSSS) modulation. It is assumed that all nodes communicate using the same transmission power. Additionally all links are considered to be symmetric and have the same link gain in both directions. The link gain is assumed to be constant over the time slot. A packet transmission from node i to node j is considered to be successful if and only if the signal-to-noise-plus-interference-ratio (SNIR) for the link (i, j) is greater than β . We refer to the SNIR of link (i, j) as $\xi_{i,j}$. Equation 3.1 is used to determine the success of a packet transmission on the link from node i to node j .

$$\xi_{i,j} = \frac{P_r(i)N_{i,j}T_c}{N_0 + \sum_{\forall k \neq i} P_r(k)T_c} > \beta \quad (3.1)$$

In Equation 3.1, $P_r(i)$ is the received signal power at node j from node i , and $P_r(k)$ is the receive signal power at node j from interfering node k . The spreading factor used on link (i, j) is denoted $N_{i,j}$. The chip duration is T_c , and N_0 is the interference caused by Gaussian noise, both of which are assumed to be constant and the same across all links. The received signal power from node i to j is determined using Equation 3.2, where P_t is the transmission power, $d_{i,j}$ is the distance between the transmitter and the receiver, λ is the signal wavelength, and α is the path loss exponent.

$$P_r(i) = P_t \left(\frac{\lambda}{4\pi d_{i,j}} \right)^\alpha \quad (3.2)$$

3.2 Neighbors

There are two different SNIR thresholds that are used when determining the neighbors of a node. For the investigations reported in this thesis, Equation 3.2 is used to determine the received power. Hence, it is equivalent to express the SNIR threshold in terms of distance or range. However, the system design does not depend on the specific form of this equation, and any model for path loss can be employed. The first SNIR threshold defines the detectable range, referred to as R_D , which is defined as the theoretical maximum $d_{i,j}$ at which a packet could be successfully received on link (i, j) with no interference or fading and the maximum spreading factor. It is reasonable to assume that control packets between two such nodes could be exchanged using a slower, more reliable data rate, but not all links in the detectable range should be relied on for user data transfer.

The communicable range, denoted R_C , is a shorter distance than the detectable range, and nodes within the communicable range of one another can reliably transmit and receive in the presence of limited MAI. The SNIR of a transmission must exceed β for the transmission to be successful. The communicable range is the distance $d_{i,j}$ that satisfies Equation 3.3, which uses the same assumptions made for determining the detectable range.

$$\frac{P_t (\lambda/(4\pi d_{i,j}))^\alpha N_{max} T_c}{N_0} = \Omega\beta \quad (3.3)$$

The factor Ω creates a margin above the β threshold that the SNIR must satisfy. Note that the communicable range decreases as Ω increases, if all other factors are held constant. The factor takes a value in the range $1 \leq \Omega \leq 2$. Because R_C must be less than R_D , Ω cannot be less than one. If Ω is too large the communicable range becomes very short, which results in many hops being necessary to relay a packet from source to destination.

Nodes i and j are called communicable neighbors if $d_{i,j} < R_C$ and are referred to as detectable neighbors if $R_C \leq d_{i,j} < R_D$. Node i 's *neighborhood*, denoted $N(i)$, consists of node i itself and all of its 1-hop and 2-hop neighbors. Any node j is a 1-hop neighbor of node i if $d_{i,j} < R_D$, and any node k is a 2-hop neighbor of i if node k is a 1-hop neighbor of any 1-hop neighbor of i .

3.3 Lyui's Algorithm

		Candidate Slot Number															
		1	2	3	4	5	6	7	8	9	10	11	12	13	14	15	16
Color Number	1	x	x	x	x	x	x	x	x	x	x	x	x	x	x	x	x
	2		x		x		x		x		x		x		x		x
	3			x				x				x				x	
	4				x				x				x				x
	5					x								x			
	6						x								x		
	7							x								x	
	8								x								x

Table 3.1: Candidate slot numbers based on color number

Lyui's scheduling algorithm, first described in [9], requires a node to have a positive color number different from all other nodes in its neighborhood. The ideal node coloring is known to be an NP-complete problem, but there are many different distributed methods for producing a coloring that is reasonably close to optimal for an arbitrary graph. Once the nodes have been colored node i can determine the slots in which it can transmit simply by knowing the color number of each node in its neighborhood. As described in [10], node i with color number c_i is a candidate to transmit in slot t if either Equation 3.4 or 3.5 holds. Where $p(c_i)$ is the smallest power of two greater than or equal to c_i . Candidate transmission slot numbers for the first eight color numbers are marked with an 'x' in Table 3.1.

$$t = c_i + n \cdot p(c_i) \quad \text{for } n = 0,1,2\dots \quad (3.4)$$

$$t \bmod p(c_i) = c_i \bmod p(c_i) \quad (3.5)$$

Node i uses Equation 3.4 or 3.5 to determine which nodes in $N(i)$ are candidates in slot t . The candidate nodes determined by node i for slot t are referred to as $C(t, i) \subseteq N(i)$, and for any node $m \in N(i)$, $m \in C(t, i)$ if $t \bmod p(c_m) = c_m \bmod p(c_m)$. Node i transmits in slot t if $i \in C(t, i)$ and $c_i > c_m \forall m \in C(t, i)$.

The resulting schedule from Lyui's algorithm has the following properties. First if a node transmits no other node in its neighborhood can transmit in the same slot. Even though multiple color numbers are candidates, only the node with the highest color number can transmit, and the coloring algorithm guarantees that a node has a unique color number from all other nodes in its neighborhood. Secondly each node's frame length is equal to $p(c_l)$ where c_l is the largest color number in the node's neighborhood. Finally each node is guaranteed to have the opportunity to transmit at least once in its frame, as node i will always be the candidate with the largest color number in slot $t \bmod p(c_l) = c_i$.

3.4 Adaptive Transmission

Node i has the ability to reduce the spreading factor used to transmit to any neighbor j if the estimated SNIR of link (i, j) , called $\hat{\xi}_{i,j}$, is great enough. The largest spreading factor any node in the network can use is N_{max} . When N_{max} is used by node i as the spreading factor for a transmission, i may only transmit one packet in a slot. When $\hat{\xi}_{i,j}$ exceeds a threshold, i may reduce the spreading factor used on (i, j) up to a factor of four, as shown in Table 3.2.

It is assumed that receiver nodes are provided with an estimated SNIR measure on both successful and unsuccessful transmissions. Since the SNIR of a received packet is dependent on the spreading factor used for the transmission, the estimate SNIR values are multiplied by $N_{max}/N_{i,j}$ to normalize them. These values are then passed to the transmitter through acknowledgments (acks). Only the transmitter uses the estimated SNIR measures. Even though the links are symmetric, the transmitter and receiver may experience different MAI environments on average.

SNIR Estimate Threshold	Spreading Factor	Link Rate
$\beta < \hat{\xi}_{i,j} \leq 2\Omega\beta$	N_{max}	1 packet/slot
$2\Omega\beta < \hat{\xi}_{i,j} \leq 4\Omega\beta$	$\frac{N_{max}}{2}$	2 packets/slot
$4\Omega\beta < \hat{\xi}_{i,j}$	$\frac{N_{max}}{4}$	4 packets/slot

Table 3.2: Spreading factors used for different mean SNIR estimates

Reducing the spreading factor by a factor of two results in a link rate twice as fast but also reduces the SNIR as determined by Equation 3.1 by a factor of two. When the spreading factor is reduced, it is desired for the mean SNIR to still exceed the threshold of $\Omega\beta$ so that link performance is not significantly degraded. This requires the mean SNIR, $\hat{\xi}_{i,j}$, to be k times greater than $\Omega\beta$ for $N_{i,j}$ to be reduced by a factor of k .

Chapter 4

Methods for Handling Variable Fading Effects

In this chapter we describe the fading model, and how it impacts the overall all channel model. We also describe how the system is modified to improve performance in the presence of fading. A method for controlling the adaptive transmission protocol is described, and modifications are presented to improve the link metrics used for routing so they better reflect the effects of fading.

4.1 Fading Model

The log-normal fading model is used to create variability in link performance from slot to slot. A block fading model is used so that the fading environment is constant throughout the length of a slot, and it is assumed that the fading effects on a link are independent from slot to slot. Note that in this section the term link is used to describe the physical interaction between two nodes and does not indicate the existence of a graph edge between the two nodes. The log-normal fading model results in an additive dB gain on the received power of a transmission, which is defined as X_σ . The random variable X_σ has a Gaussian distribution with a mean of zero and a standard deviation of σ given in dB.

The fading gain on link (i, j) is given by $\chi_{i,j}$, and is converted from dB by Equation 4.1.

$$\chi_{i,j} = 10^{X_\sigma/10} \quad (4.1)$$

The fading gain for each link is drawn independently for each slot. In this investigation we assume a fixed network topology. Each link is assigned a σ value to represent the log-normal fading for that link. The distribution for assigning σ values is given in Chapter 6.

The channel model as described by Equation 3.1 is modified by including $\chi_{i,j}$ to account for fading. With fading the SNIR of a transmission is calculated using Equation 4.2, and the SNIR still must exceed β for the transmission to be successful. The received power of both the transmitting and interfering nodes are impacted by the fading model based on the individual log-normal fading variables.

$$\xi_{i,j} = \frac{P_r(i)\chi_{i,j}N_{i,j}T_c}{N_0 + \sum_{\forall k \neq i} P_r(k)\chi_{k,j}T_c} > \beta \quad (4.2)$$

4.2 Transmission Success Probability Link Rate Control

The ability for nodes to reduce the spreading factor of links allows for faster data rates and better network performance but also results in the SNIR of transmissions falling closer to the β threshold making the transmissions more likely to fail. When the estimated SNIR measures are fairly constant from one slot to the next the adaptive transmission protocol works well without causing many transmission failures. In the presence of fading, link quality varies from slot to slot and makes mean SNIR a less reliable measure for setting link transmission rates.

Input:Link transmission success probability $\rho_{i,j}$ Mean estimate SNIR $\hat{\xi}_{i,j}$ Current link spreading factor $N_{i,j}$ Boolean $RateLock_{i,j}$ ▷ Either *Locked* or *Unlocked***Output:**New link spreading factor $\hat{N}_{i,j}$ 1: **if** $RateLock_{i,j}$ is *Unlocked* **then**2: $\hat{N}_{i,j} = \text{BESTSPREADINGFACTOR}(\hat{\xi}_{i,j})$ 3: **else**4: $\hat{N}_{i,j} = N_{i,j}$ 5: **if** $\rho_{i,j} \leq P$ **then**6: $\hat{N}_{i,j} = \min(N_{max}, 2\hat{N}_{i,j})$ 7: $RateLock_{i,j} = \text{Locked}$ 8: **function** $\text{BESTSPREADINGFACTOR}(\hat{\xi})$ 9: **if** $\hat{\xi} \leq \Omega\beta$ **then**10: Return N_{max} 11: **else**12: //Largest Power of 2, N_2 , such that $\hat{\xi} > N_2\Omega\beta$ 13: $N_2 = 2^{\lceil \log_2(\hat{\xi}/(\Omega\beta)) \rceil}$ 14: Return $N_{max}/\min(4, N_2)$

Figure 4.1: Transmission Success Probability link rate control pseudo-code

A measure of the transmission success probability of a link (i, j) can be used to determine if the fading environment is causing transmissions to fail. Transmitter i can determine the transmission success probability of link (i, j) by counting the number of received link acks from node j divided by the total number of transmissions sent to node j .

The measured transmission success probability, $\rho_{i,j}$, is compared to the given transmission success probability threshold, P , as shown in Figure 4.1. If the measured success probability falls below the threshold probability, then a higher spreading factor is selected for the link. The higher spreading factor results in a link that is more resistant to fading.

If the link rate is unlocked, the spreading factor is selected using the process described in Section 3.4. Once a link rate is reduced and locked, it cannot be increased again. This avoids oscillating between states of good and poor link performances. There is no method for unlocking the link rate. For the investigations reported in this thesis, the network topology and fading levels are assumed to be fixed. An adaptive protocol to respond to changes in topology or fading levels is outside of the scope of this thesis. Once the link rate is locked it remains locked for the life time of the network. While the link rate can not be increased once it is locked, it can be reduced further until a rate of one packet per slot is reached. This could be necessary to decrease transmission failures on links heavily impacted by fading.

4.3 Routing Metrics

We investigate multiple routing metrics with the goal of finding a metric that performs well in the presence of fading. In this section we describe the different routing metrics.

SNIR

A routing metric similar to the one described in [4] is used as the base case to compare the performance of different routing metrics. It uses several factors to determine link weights. The cost of the link (i, j) is determined by Equation 4.3. Let $SOR(j)$ denote the slot ownership rate of node j . This is defined as the fraction of slots assigned to j according to Lyui's algorithm, and is calculated as the number of slots assigned to j divided by the frame length of j . Define $LinkRate_{i,j}$ as the number of packets that can be transmitted over link (i, j) in a single slot, and it is calculated as $N_{max}/N_{i,j}$. Notice

$LinkRate_{i,j}$ is dependent on the average estimated SNIR of link (i, j) .

$$Cost_{i,j} = \frac{\xi(\hat{\xi}_{i,j})(1 + U_j)}{SOR(j) \times LinkRate_{i,j}} \quad (4.3)$$

The utilization factor of node j is U_j , and it takes values between 0 and 1. The value for U_j is updated in each slot t assigned to node j using Equation 4.4, where $T(t, j)$ indicates the fraction of slot t in which node j transmits. Node j determines $T(t, j)$ by summing the inverses of the link rates used for each transmission in slot t . If node j has two packets to transmit, one to node i with a link rate of two packets per slot, and one to node k with a link rate of four packets per slot, then $T(t, j) = 1/2 + 1/4 = 3/4$. However, if node j had a third packet also being sent to k , then $T(t, j) = 1/2 + 1/4 + 1/4 = 1$. The utilization factor gives neighbors with a higher load a larger weight. This helps to evenly distribute traffic amongst the nodes in the network.

$$U'_j = (0.95) \cdot U_j + (0.05) \cdot T(t, j) \quad (4.4)$$

A link with a low mean SNIR is more susceptible to failed transmissions due to MAI and fading effects. The function $\xi(x)$ penalizes a node with low mean SNIR, and is shown in Equation 4.5. The threshold $\Omega\beta$ is the value that the mean SNIR of (i, j) must exceed for nodes i and j to be considered communicable neighbors. Transmissions over link (i, j) have a high probability of success when there is no fading present if $\hat{\xi}_{i,j} > \Omega\beta$. Nodes i and j are detectable neighbors if $\beta < \hat{\xi}_{i,j} < \Omega\beta$. These links are used for routing when necessary, to aid in network connectivity. The cost of these links increases exponentially as the SNIR decreases, so other links are likely to be chosen when available.

$$\xi(x) = \begin{cases} \infty & x \leq \beta \\ 1 - \ln\left(\frac{x - \beta}{\Omega\beta - \beta}\right) & \beta < x \leq \Omega\beta \\ 1 & x > \Omega\beta \end{cases} \quad (4.5)$$

ETX

The goal of the ETX routing metric, first described in [5], is to reduce the total number of transmissions needed to relay a packet from source to destination. This includes the number of times a packet has to be retransmitted over the same link. This is done by setting the cost of link (i, j) equal to the expected number of transmissions for a single packet over (i, j) as shown in Equation 4.6. The ETX metric is originally described in terms of d_f and d_r which are the success probability of a packet in the forward direction and a packet in the reverse direction (an ack) respectively. The ETX metric is also commonly calculated in terms of e_p , the probability that a packet transmission fails, but the two calculations yield the same result.

$$Cost_{i,j} = \frac{1}{1 - e_p} = \frac{1}{d_f \times d_r} = ETX_{i,j} \quad (4.6)$$

While the ETX routing metric helps avoid links where a high number of retransmissions are necessary, it is very simple and offers little if link performance is very good. It is easy to see that when there are no packet errors for a link the ETX is always equal 1. This results in a routing metric very close to minimum hop routing when links are good, which is well known to have poor performance [22].

SNIR.ETX

The SNIR.ETX link metric includes the ETX metric as a multiplicative cost on the SNIR metric. The SNIR metric distributes traffic efficiently when links perform well, and the ETX measure avoids the links which perform poorly. The SNIR.ETX routing metric is calculated using Equation 4.7. When links are very good on average the SNIR.ETX routing metric approaches the same weight as the SNIR metric. For example, if an adaptive transmission protocol is added to maintain high link success rates, then there are few transmission failures. In this scenario, including the ETX metric as a factor does not have

much of an impact on selecting routes.

$$Cost_{i,j} = \frac{\xi(\hat{\xi}_{i,j})(1 + U_j)ETX_{i,j}}{SOR(j) \times LinkRate_{i,j}} \quad (4.7)$$

SNIR.StdDev

The link metric, SNIR.StdDev, also modifies the SNIR metric with the objective of reducing the number of failed transmissions. It uses a heuristic based on the standard deviation of the estimated SNIR measures to avoid links that exhibit a high level of variance in the SNIR, such as due to high levels of fading. The heuristic weight of link (i, j) is defined as $StdDev_{i,j}$ and is calculated using Equation 4.8.

$$StdDev_{i,j} = (1 + \hat{\xi}_{i,j} - \hat{\sigma}_{i,j}) \quad (4.8)$$

The standard deviation of the estimated SNIR values is defined as $\hat{\sigma}_{i,j}$. The value of $StdDev_{i,j}$ decreases as the difference between the mean SNIR and standard deviation value decreases, and the resulting SNIR.StdDev metric is given by

$$Cost_{i,j} = \frac{\xi(\hat{\xi})_{i,j}(1 + U_j)}{SOR(j) \times LinkRate_{i,j} \times StdDev_{i,j}} \quad (4.9)$$

Chapter 5

Simulation Details

In this chapter we describe the implementation of the simulation, and discuss the assumptions used for the experiments. We explain how nodes are positioned in the simulated field and how links are formed between the nodes. We describe how network traffic is generated and how transmissions within a single time slot are processed.

5.1 Initialization of Network

The network consists of n nodes which are placed on a square field that is described by the *FieldLength*, the length of one side of the square. Nodes are located in the field by a Cartesian, (x, y) , coordinate. The x and y coordinates in each pair are determined from independent uniform random variables. A desired detectable range, R_D , is given and then the transmission power, P_t , is calculated. The transmission power is determined using Equation 5.1, which is found by substituting Equation 3.2 into Equation 3.1 and solving for P_t . The detectable range is set to be 200m in the simulation.

$$P_t = \left(\frac{4\pi R_D}{\lambda} \right)^\alpha \frac{\beta N_0}{T_c N_{max}} \quad (5.1)$$

A shorter communicable range is chosen to provide a set of links that are more resistant to the effects of MAI. The distance R_C should be set as the largest distance less than

R_D that results in good protection from MAI. Selecting a very small communicable range results in many hops being required to relay packets and can decrease network performance. Preliminary testing showed that a communicable range of 187m with a detectable range of 200m results in nearly no packets being dropped due to multiple-access interference. The SNIR threshold, Ω , is calculated to set the given communicable range, and nodes i and j are communicable neighbors if Equation 5.2 holds on average for link (i, j) . Note that interference from all nodes is considered. Because transmissions are scheduled using Lyui's algorithm, none of the interferers are one-hop neighbors of the receiver.

$$\xi_{i,j} = \frac{P_r(i)N_{i,j}T_c}{N_0 + \sum_{\forall k \neq i} P_r(k)T_c} > \Omega\beta \quad (5.2)$$

Solving for Ω in the special case with no MAI or fading, a spreading factor of N_{max} , and $P_r(i)$ (see Equation 3.2) with $d_{i,j} = R_C$ and P_t set for the given detectable range, yields Equation 5.3.

$$\Omega = \frac{P_t (\lambda/(4\pi))^\alpha N_{max}T_c}{\beta N_0} \quad (5.3)$$

Each pair of nodes in the network is assigned a fading environment, even if the two nodes are not neighbors. The fading environment is defined by the σ value of the log-normal variable, and the fading between the two nodes is the same in both directions. The σ value for each pair is randomly and uniformly distributed over a given range of σ_{min} dB to σ_{max} dB, and it is assumed that the σ values for any two pair of nodes are statistically independent.

A wireless link (i, j) is established for any pair of nodes i and j that are detectable neighbors. The set of nodes that are communicable neighbors of node i is a subset of node i 's detectable neighbors so a wireless link exists for all communicable neighbors as well. If after all the links in the network have been established, the network is disconnected (i.e. there exists one or more pair of nodes for which no route can be formed between them)

then the simulation is terminated and a new random graph is generated.

5.2 Traffic Generation and Routing

Data packets are generated randomly in the network. The packet arrival rate, denoted γ , is defined as the average number of packets generated in the network in each slot. Each node has a probability of γ/n to generate a packet in each slot. More than one packet may be generated in the same slot, but on average γ packets are generated in a single slot. When a packet is generated, the destination is chosen from the remaining nodes by a uniform random variable. All packets are assumed to be the same size.

A node determines the next hop for a packet to reach its destination based on its routing table. Since the network is guaranteed to be connected there is a routing entry at each node for every other node in the network. The routing tables are generated using a centralized Dijkstra's algorithm along with one of the cost functions listed in Section 4.3. A centralized routing protocol is adopted for simplicity. An investigation of the dynamics of distributed routing protocols is outside the scope of this work. Link weights, routing tables, and link transmission rates are updated every 500 slots.

Each node has a local transmission buffer capable of holding 20 packets. When packets arrive at node i , either by being generated by node i or being received by node i from one of its neighbors, node i determines the packet's next hop and the current data rate used on that link. Packets are then given priority in the queue based on the data rate of their next hop. Packets using a faster data rate have higher priority and are placed closer to the head of the queue.

At the start of each time slot the set of nodes which have been assigned the current slot and have packets to transmit is determined. While in some cases nodes may not have enough packets to fill an entire slot, it is assumed that once a node begins transmitting it will continue to transmit throughout the slot. When a packet is transmitted the fading gains between the packet's receiver and all other transmitting nodes are determined

based on the log-normal variable for each pair of nodes. The fading gain values remain constant throughout the slot. A transmission is considered successful if the SNIR satisfies Equation 4.2.

We use a similar approach as described in (Cite paper here) to select multiple packets for a transmission. For example, assume node i can transmit four packets, using $N_{max}/4$ as the spreading factor. Furthermore, assume two of the packets are for node j and the other two for node k . It is possible for the transmission to k to be successful while the transmission to node j fails. If the transmission to a neighbor is successful, then all the packets in that transmission are delivered to that neighbor. Likewise, if a transmission fails none of the packets are delivered.

5.3 Network Performance Measures

In order to collect measures of the steady state network performance, the network runs a 10,000 slot warm-up without tracking network performance measures. This allows for transmission queue lengths to stabilize. After the warm-up period network measures are tracked for 100,000 slots, and the resulting network measures are averaged over 200 random networks, not counting disconnected networks.

The end-to-end delay is a measure of the amount of time it takes for packets to go from source to destination on average. It is calculated as the difference between the slot number in which a packet reaches its destination and the slot number in which it was generated. Network throughput is the measure of the number of packets that successfully reach their destinations per slot. The percent of packets dropped and the total number of packets dropped are also provided as measures of network performance.

There are two scenarios in which a packet can be dropped. The first way a packet can be dropped is referred to as a re-transmission drop. If the SNIR of the transmission is too low to allow successful decoding of the packet, the transmission fails. This can be caused by a combination of MAI and the effects of the fading environment. When the

receiver determines that the transmission is unsuccessful it sends an acknowledgment back to the transmitter. This acknowledgment is assumed to happen immediately and is always successful. In this case the packet is re-queued for transmission in a future slot. Each packet is marked with the number of times its transmission fails, and if the count of failures reaches six the packet is dropped from the network. If the packet transmission is successful the failed transmission count is reset to zero before forwarding the packet again.

Secondly a packet is dropped if the receiving node's transmission buffer is full, or the transmission buffer of the source node is full when the packet is generated. In this case the packet is dropped immediately and no attempt to retransmit it is made. We refer to this event as a buffer overflow.

Chapter 6

Results

In this chapter we evaluate the performance of the system in the presence of fading. We show that log-normal fading reduces the overall performance of the system. We show the impacts of the transmission success probability (TSP) link rate control protocol described in Section 4.2. We show that using transmission success probabilities, as a measure of link quality, is an effective way to control the adaptive transmission protocol in the presence of fading. We evaluate the different routing metrics listed in Section 4.3, and we show how these routing metrics impact the performance of the system with TSP. Table 6.1 defines key parameters which are used for all results in this section. For parameters in Table 6.2, the values used in the initial studies are listed. We also present results that consider different network densities, fading levels, and P values for the TSP protocol. The transmission success probability threshold, P , is defined in Section 4.2 and is the threshold at which link rates are lowered.

Parameter	Default Value
α	3
β	8
λ	0.125m
T_c	$2.9e-7$ s/chip
N_0	$4.0e-21$ J/Hz
N_{max}	64 chips/symbol
<i>NumberofNodes</i>	500
R_D	200m
R_C	187m

Table 6.1: Unchanged network parameters

Parameter	Default Value
Field Length	2000m
Fading	0-5dB
P	0.7

Table 6.2: Default parameters that may be changed

The level of fading for a simulation scenario is given as a range of the standard deviations that the log-normal variables for each link in the network may have in dB. For the initial simulation results, the σ value of the log-normal variable for each link is randomly and uniformly distributed over the range 0 to 5dB.

We define a performance threshold for comparing network performance in terms of the percentage of packets dropped. We define Γ as the largest arrival rate γ such that for all $\gamma < \Gamma$ the percentage of packets dropped is less than 10%. System performance can then be compared in terms of Γ .

All graphs in this chapter, unless stated otherwise, compare different combinations

of routing metrics and TSP to a base case which is designated with the "No Fading" label. Adaptive transmission is used for all test cases unless stated otherwise. The system uses the SNIR routing metric as described in Section 4.3 in the no fading case, and TSP is not enabled. Link rates are never locked in the no fading case. The other lines in the graphs show the system performance in the presence of fading. The labels show which routing metrics are used, and "+ TSP" indicates that TSP is enabled. The results labeled SNIR show how the unmodified system performs in the presence of fading.

6.1 Performance of TSP Link Rate Control

The variance in link quality as a result of the log-normal fading model is easily shown to have a significant negative impact on network performance. In Figure 6.1 the SNIR curve shows that the original system drops a large percentage of the generated packets when subjected to fading, as even at the lowest packet arrival rates approximately 20% of packets are dropped. However, the addition of the TSP link rate control protocol to the SNIR routing metric can significantly improve the performance of the system when fading is present. The results for SNIR.ETX and SNIR.ETX + TSP show that making adjustments to the routing protocol that work with the TSP protocol further improve the performance gains.

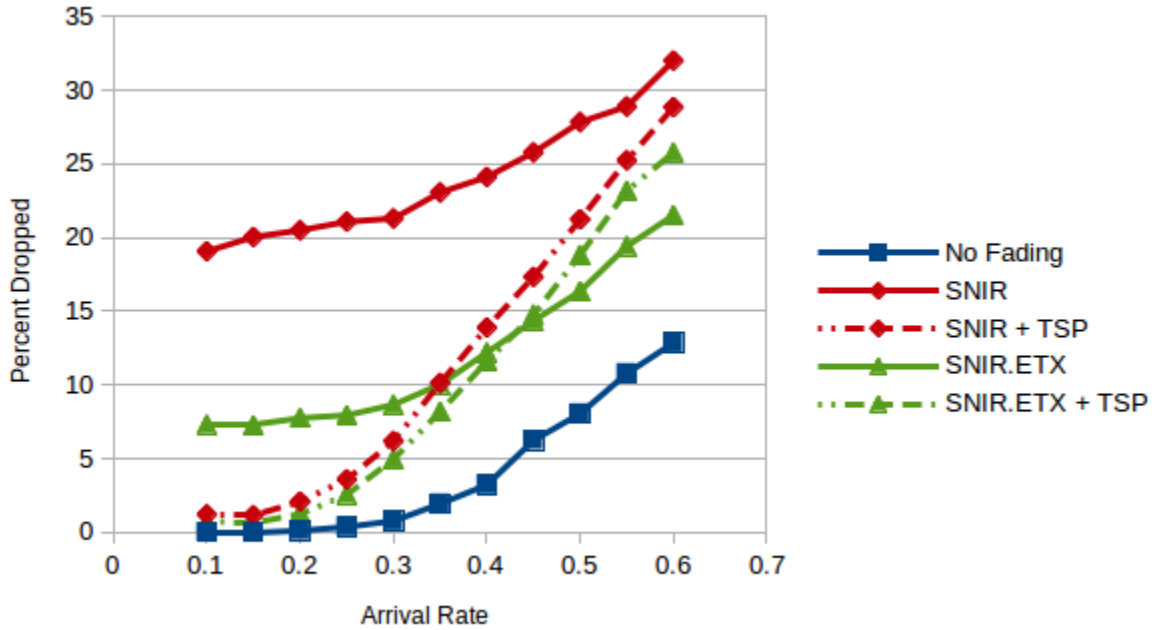


Figure 6.1: Percent Dropped vs. Arrival Rate for: No Fading, SNIR, SNIR.ETX, SNIR + TSP, and SNIR.ETX + TSP

In the presence of fading the performance is so poor that there are no γ at which the percentage of packets dropped is below the threshold of 10% for the original SNIR routing metric. When the routing metric is modified to include ETX with the SNIR metric, testing shows that the system performs much better than the with the SNIR routing metric. The SNIR.ETX routing metric results in a Γ value approximately 0.2 packets/slot lower than Γ in the no fading case. While performance is still noticeably worse than when there is no fading present, the results still show roughly a 50% reduction in dropped packets compared to the SNIR metric. Using the TSP protocol to better control the adaptive transmission protocol further improves the performance with the SNIR.ETX metric by increasing Γ by approximately 0.05 packets/slot. More significantly, the TSP protocol improves the performance with the SNIR.ETX metric for $\gamma < \Gamma$. The TSP protocol also shows significant

improvements when used with the original SNIR metric, but combining the TSP protocol with the SNIR.ETX metric shows slightly better performance. It is worth noting that the SNIR.ETX metric out performs SNIR.ETX + TSP, but only at higher packet generation rates. However, at the higher generation rates, the percentage of packets dropped exceeds the performance threshold.

There is often interest in how the system performs in terms of the network throughput measure. Figure 6.2 shows how the trends in percentage of packets dropped translate to network throughput. The fading model causes a noticeable reduction in the network throughput when no attempt is made to address the problem. Improving the system with a better routing metric and the addition of the TSP protocol results in higher throughput in the presence of fading, but the difference in throughput of these improved protocols is negligible. The SNIR.ETX metric performs slightly better at higher arrival rates, but this is only for $\gamma > \Gamma$. This is the same observation found when investigating the percent dropped measure. For the remainder of the chapter we use the percent of packets dropped as the primary measure of network performance, because it better illustrates the performance gains at lower packet generation rates.

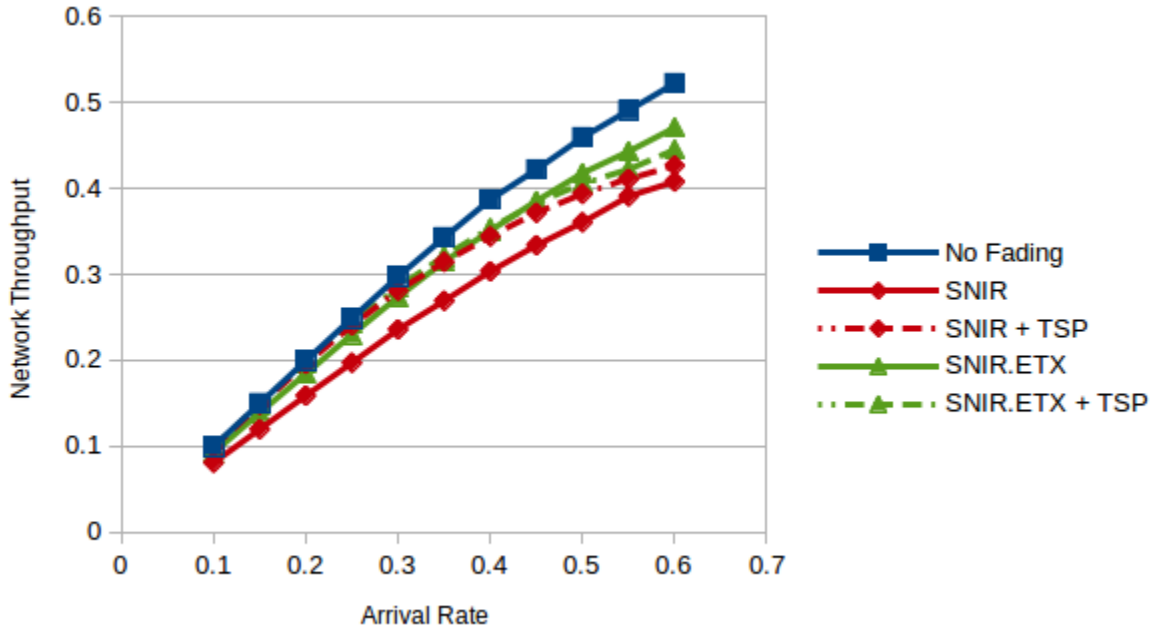


Figure 6.2: Throughput vs. Arrival Rate for: No Fading, SNIR, SNIR + TSP, SNIR.ETX, and SNIR.ETX + TSP

Figure 6.3 shows that, while the TSP protocol is able to reduce the percentage of packets dropped, it comes at the cost of higher end-to-end delay. This is not surprising since the main function of the TSP protocol is to reduce the transmission rate of certain links, which reduces the number of packets that can be transmitted on a link in a single slot. This increase in delay becomes more substantial as the packet arrival rate increases. However, the main point of interest is still $\gamma < \Gamma$. The delay measure can also be misleading when there are a large number of dropped packets, because the delay is measured only for the fraction of packets that make it to their destinations. Furthermore, a packet is more likely to reach its destination if it requires fewer relays, which often reduces the delay. It is clear that the TSP protocol causes an increase in end-to-end delay, but this is offset by the increase in throughput and decrease in the number of dropped packets.

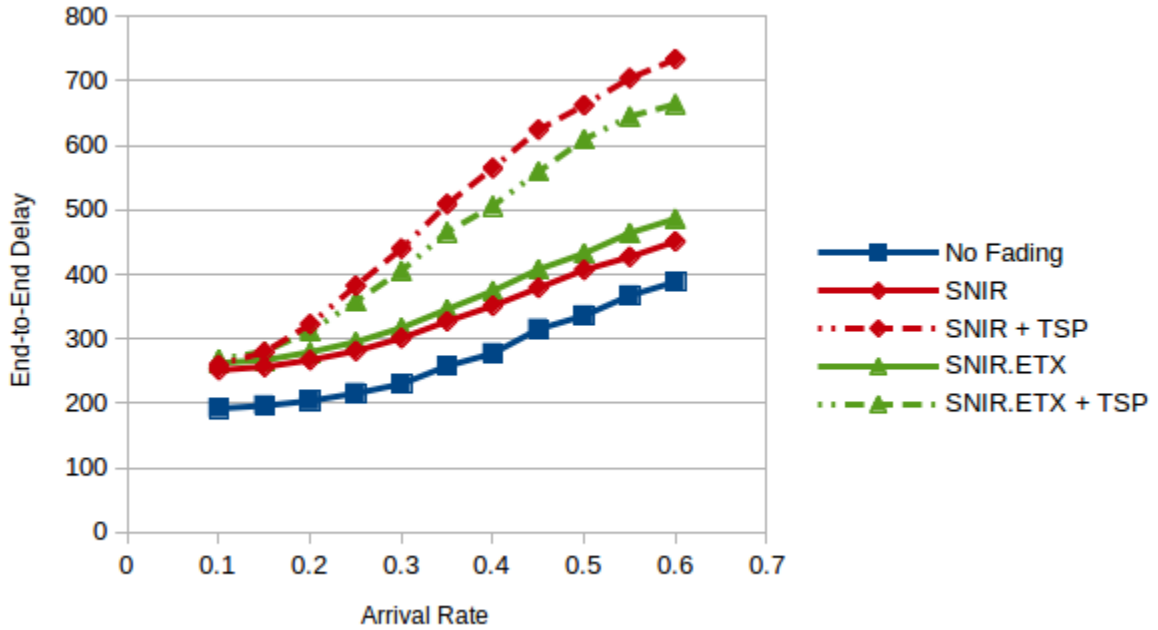


Figure 6.3: End-to-End Delay vs. Arrival Rate for: No Fading, SNIR, SNIR + TSP, SNIR.ETX, and SNIR.ETX + TSP

6.2 Importance of Investigating the Routing Metric With the TSP Protocol

The TSP protocol shows significant improvement in network performance without any changes to the routing metric. However, it is critical that the TSP protocol is combined with an appropriate routing metric. In the following experiments we investigate the performance of the TSP protocol in combination with Min Hop, the ETX routing metric, and a routing metric that makes decisions based on the estimated standard deviation of the SNIR for a link.

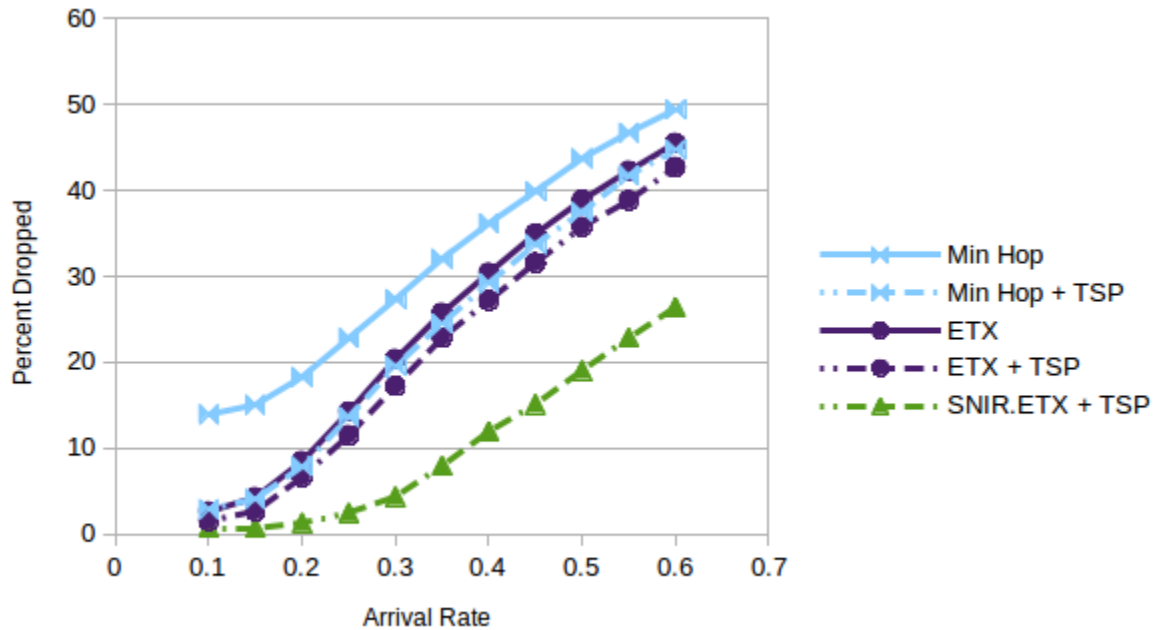


Figure 6.4: Percent Dropped vs. Arrival Rate for: Min Hop, Min Hop + TSP, ETX, ETX + TSP, and SNIR.ETX + TSP

Figure 6.4 shows how the TSP protocol impacts the percentage of packets dropped for Min Hop and the ETX metric. The TSP protocol significantly improves the Min Hop routing metric making the performance almost identical to the ETX metric, but the TSP protocol does not improve performance as much when added to the ETX routing metric. The TSP protocol shows only minor improvements to the ETX metric.

The SNIR.StdDev routing metric adds a multiplicative factor to the original SNIR metric based on the link's estimated standard deviation in SNIR. The original SNIR metric is modified as described in Section 4.3 to determine the cost of the link. Notice that the results for the SNIR.StdDev metric do not include the link layer modifications with the TSP protocol. Instead only the routing protocol is modified to respond to the fading environment. The SNIR.StdDev routing metric reduces the percentage of packets dropped

when fading is present. Its network performance is only slightly worse than the system that employs the TSP protocol. In particular, the Γ performance measure for the SNIR.StdDev metric is approximately 0.05 packets/slot less than SNIR.ETX + TSP.

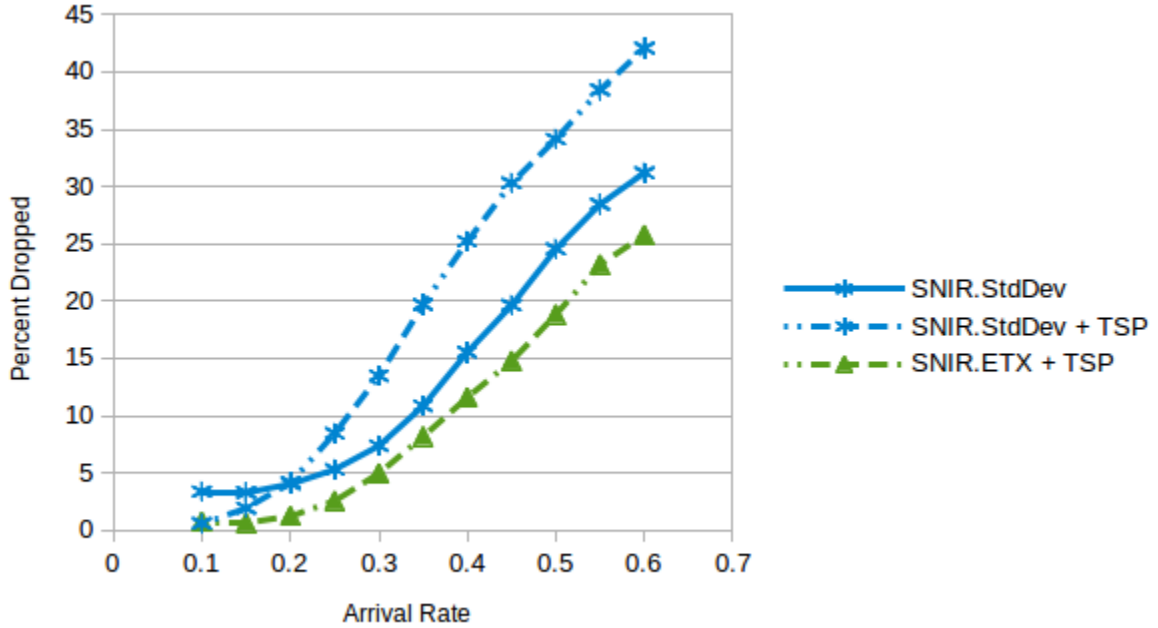


Figure 6.5: Percent Dropped vs. Arrival Rate for: SNIR.ETX + TSP, SNIR.StdDev, and SNIR.StdDev + TSP

Combining the SNIR.StdDev routing metric with the link-layer TSP protocol results in a significant increase in the number of dropped packets. Using either the routing metric or the TSP protocol is effective, but combining them leads to much poorer selection of routes. When this routing metric is combined with TSP link rate control Γ is reduced by nearly 0.1 packets/slot. It is critical to select the routing metric that complements the TSP protocol. Choosing the best routing metric without considering the TSP protocol leads to poor performance.

Next, we consider the reasons that packets are dropped. This provides additional

insight into system performance. In the simulation there are only two scenarios in which a packet can be dropped. First, a packet is dropped if the receiving node's transmission buffer is full. In this case the packet is dropped immediately and no attempt to retransmit it is made. We refer to this event as a buffer overflow. The second way a packet can be dropped is if the SNIR of the transmission is too low to allow successful decoding of the packet. This is caused by a combination of multiple access interference (MAI) and the effects of the fading environment. In this case the transmission is attempted a total of six times, and if the transmission fails on the sixth attempt the packet is dropped from the network. This second case is referred to as a re-transmission drop.

It is shown in Figure 6.6 that the original system rarely drops packets due to transmission failures in the case where there is no fading present. This suggests that the transmission scheduling algorithm is effective in controlling the effects of MAI and that the re-transmission drops in the fading environment are mainly due to the fading model. The systems which perform the best in terms of percentage of packets dropped (see Figure 6.1) balance reducing the number of buffer overflows and the number of re-transmission drops. The two systems that perform best in the presence of fading, SNIR + TSP and SNIR.ETX + TSP, actually experience more buffer overflows than SNIR and SNIR.ETX, but they have significantly fewer re-transmission drops. This shows a trade-off of adding the TSP protocol to a system. Generally the TSP protocol reduces the number of re-transmission drops at the cost of more buffer overflows.

Figure 6.7 shows the types of packet drops for the SNIR.StdDev metric. The SNIR.StdDev routing metric provides a significant improvement to the number of re-transmission drops without the aid of the TSP protocol, but it incurs roughly the same number of buffer overflows as SNIR.ETX + TSP. When the TSP protocol is added to this routing metric there is still a negative trade-off that increases buffer overflows, but since SNIR.StdDev already does a good job of reducing the number of re-transmission drops, the TSP protocol does not improve the system as much in this measure. This causes the overall performance of the system to decrease.

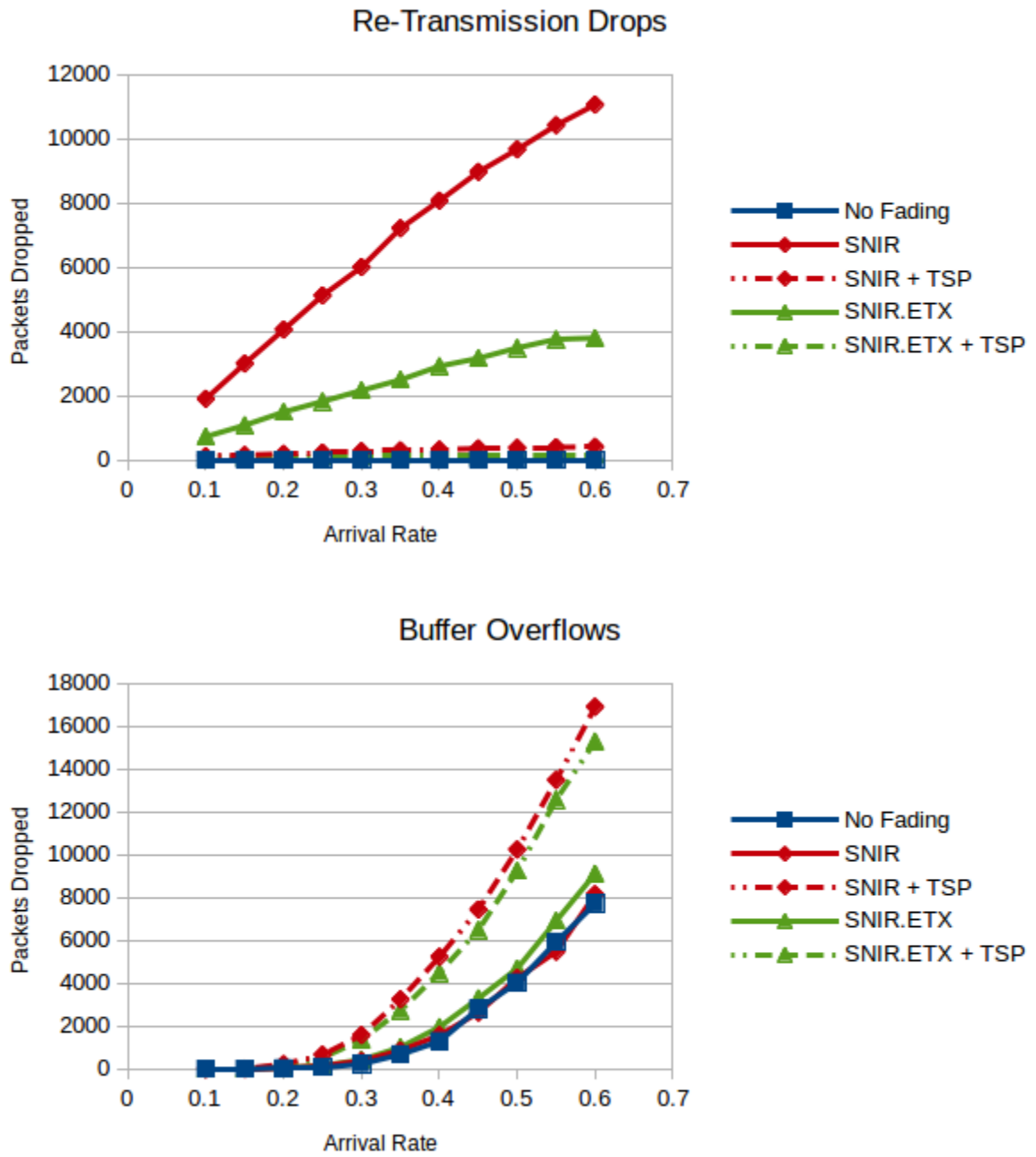


Figure 6.6: Break down of dropped packets for: No Fading, SNIR, SNIR + TSP, SNIR.ETX, and SNIR.ETX + TSP

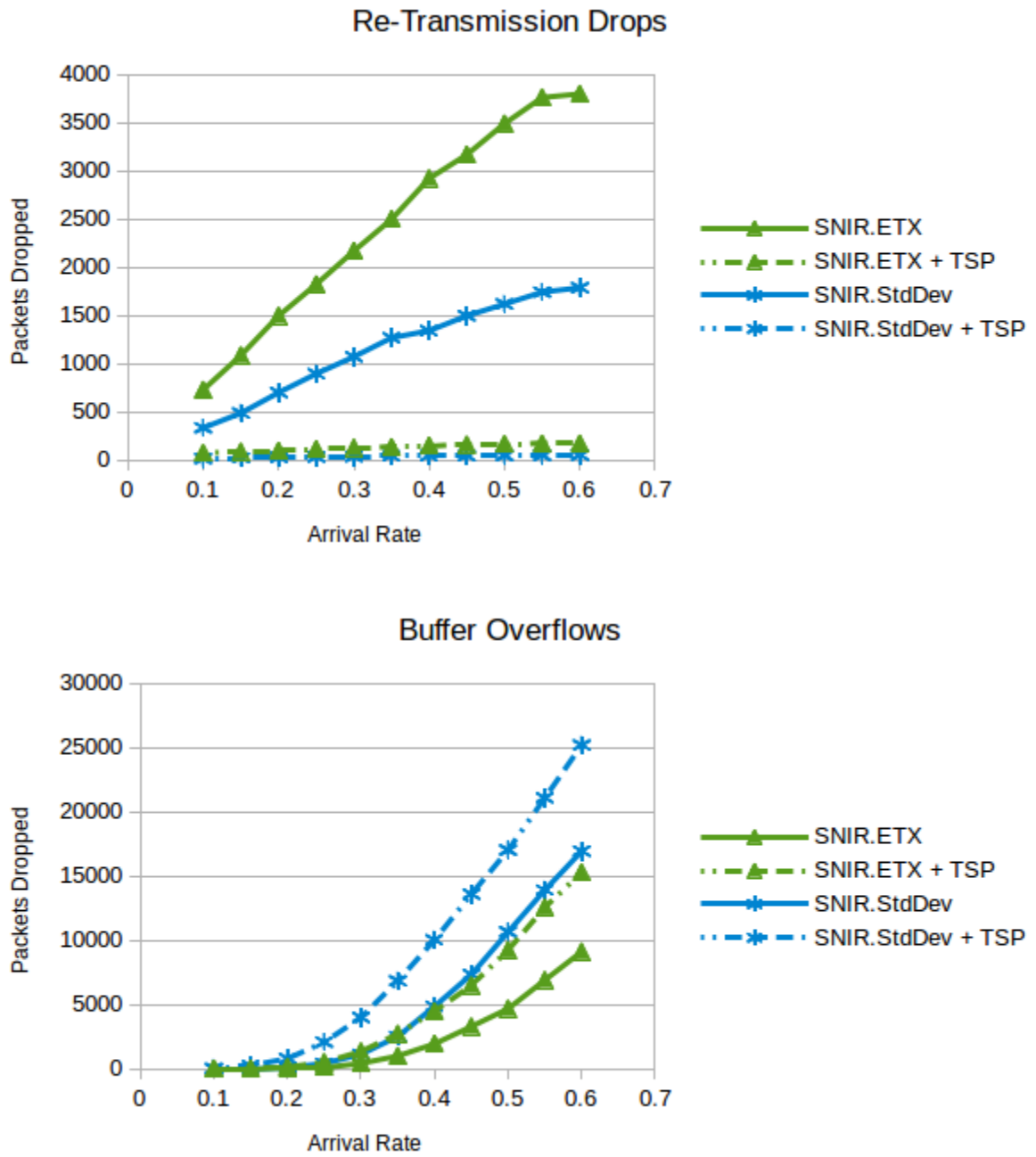


Figure 6.7: Break down of dropped packets for: SNIR.ETX, SNIR.ETX + TSP, SNIR.StdDev, and SNIR.StdDev + TSP

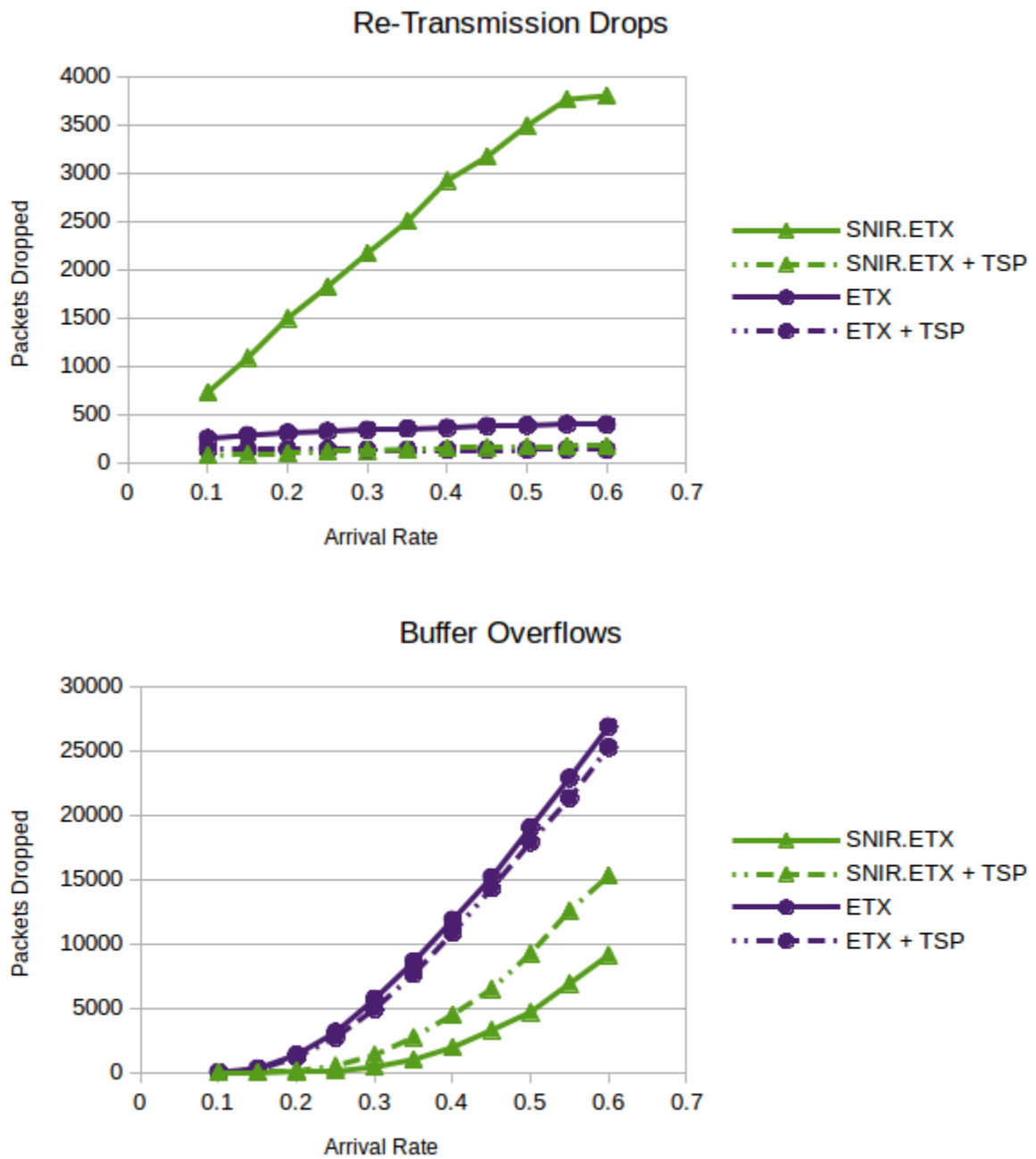


Figure 6.8: Break down of dropped packets for: SNIR.ETX, SNIR.ETX + TSP, ETX, and ETX + TSP

An examination of the types of packet drops for the SNIR.StdDev and SNIR.StdDev + TSP trials show that, when selecting a routing metric, more emphasis should be placed on finding a routing metric that addresses congestion and reduces the number of buffer overflows. Figure 6.8 shows that addressing congestion is required. The ETX routing metric reduces the number of re-transmission drops. However, unlike the SNIR.StdDev metric, when the TSP protocol is enabled there is no increase in the number of buffer overflows. This might be due to the fact that the ETX metric is poor at limiting buffer overflows due to congestion, or it could be that the routing metric is not negatively impacted by the TSP protocol. This illustrates that a cross-layer design approach must be employed to jointly design the routing metric and the link-layer adaptive transmission protocol.

6.3 Impact of the TSP Protocol Threshold

The transmission success probability threshold controls how aggressively the TSP protocol reacts to transmission failures. Recall the TSP threshold determines the minimum packet success probability that is required for a link. If the measured forwarding rate falls below the threshold the data rate on the link is reduced, if possible. While a lower data rate improves the packet success probability it also reduces the rate packets can be forwarded. A higher TSP threshold causes link rates to be reduced sooner in response to failed transmissions. In this section we examine the sensitivity of the performance of the TSP protocol with the respect to the TSP threshold. All figures in this section utilize the system with SNIR.ETX + TSP and only the TSP threshold is varied.

Figure 6.9 shows how the TSP threshold affects the percentage of packets that are dropped. The higher the TSP threshold is the lower the percentage of packets dropped for small values of γ , but as the TSP threshold is increased the performance for larger γ values starts to decrease. For TSP thresholds 0.8 and 0.9 Γ begins to decrease. For lower thresholds the performance for smaller γ is sacrificed, but performance falls off more slowly. Starting with a TSP threshold equal to 0.4, Γ starts to decrease. While the TSP threshold does

impact the percentage of packets dropped, the TSP protocol still shows better performance than SNIR.ETX (see Figure 6.1) for most threshold values.

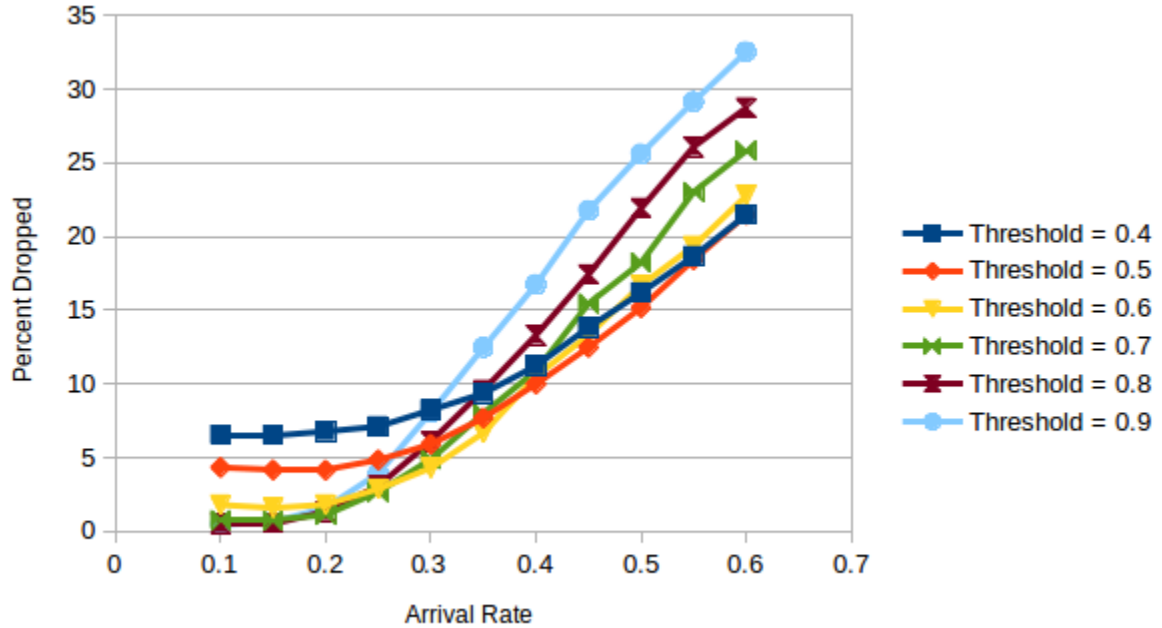


Figure 6.9: Threshold comparison of percent dropped vs. arrival rate for: TSP threshold values $\{0.4, 0.5, 0.6, 0.7, 0.8, 0.9\}$

Figure 6.10 shows how the TSP threshold impacts the network throughput. For lower arrival rates the TSP threshold has no significant impact on network throughput, and it is not until after $\gamma > \Gamma$ that the performance at different thresholds begin to separate. The reduction in throughput is also gradual for different TSP thresholds. The largest separation in throughput is only about 0.07 packets/slot, and only at high generation rates and lower packet completion rates. All selections of TSP threshold shows no reduction in throughput performance compared to SNIR.ETX in Figure 6.2, for $\gamma < \Gamma$.

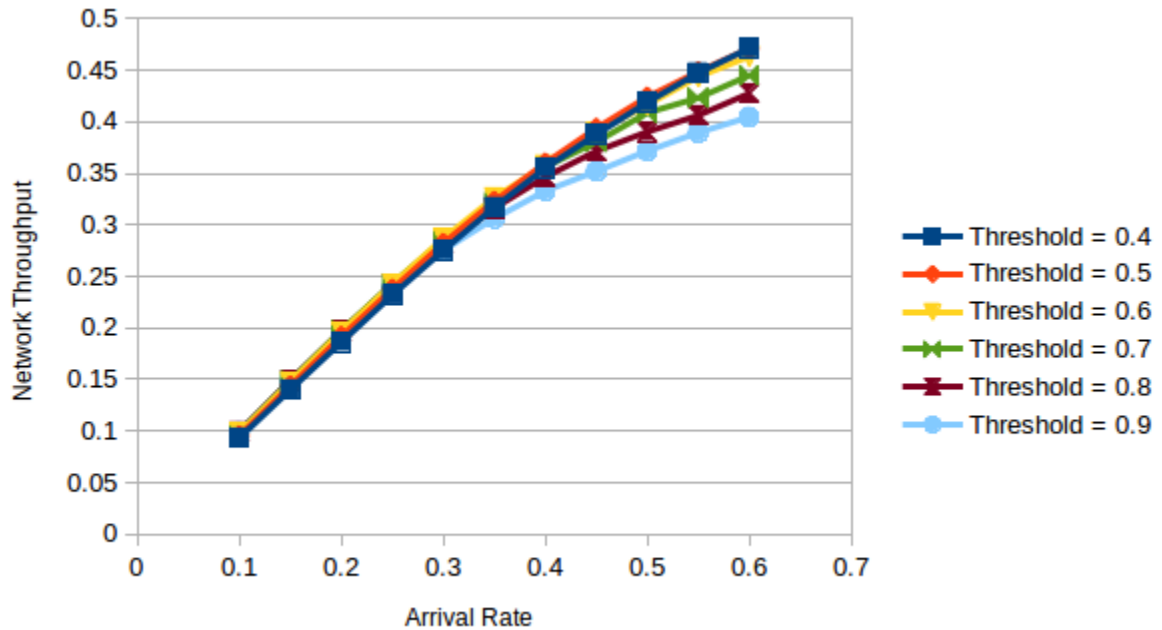


Figure 6.10: Threshold comparison of network throughput vs. arrival rate for: TSP threshold values {0.4, 0.5, 0.6, 0.7, 0.8, 0.9}

In Figure 6.11 it is shown that as the TSP threshold increases the end-to-end delay also increases. This result is expected. As is shown in Figure 6.3 the TSP protocol increases delay in general because it reduces the average transmission rate of the network. By increasing the TSP threshold, link rates are more aggressively reduced, and this causes the average transmission rate of the network to further decrease. Selecting a TSP threshold value of 0.6 results in a good compromise in performance across a wide range of packet generation rates. Notice that enabling the TSP protocol improves network performance regardless of which threshold is selected.

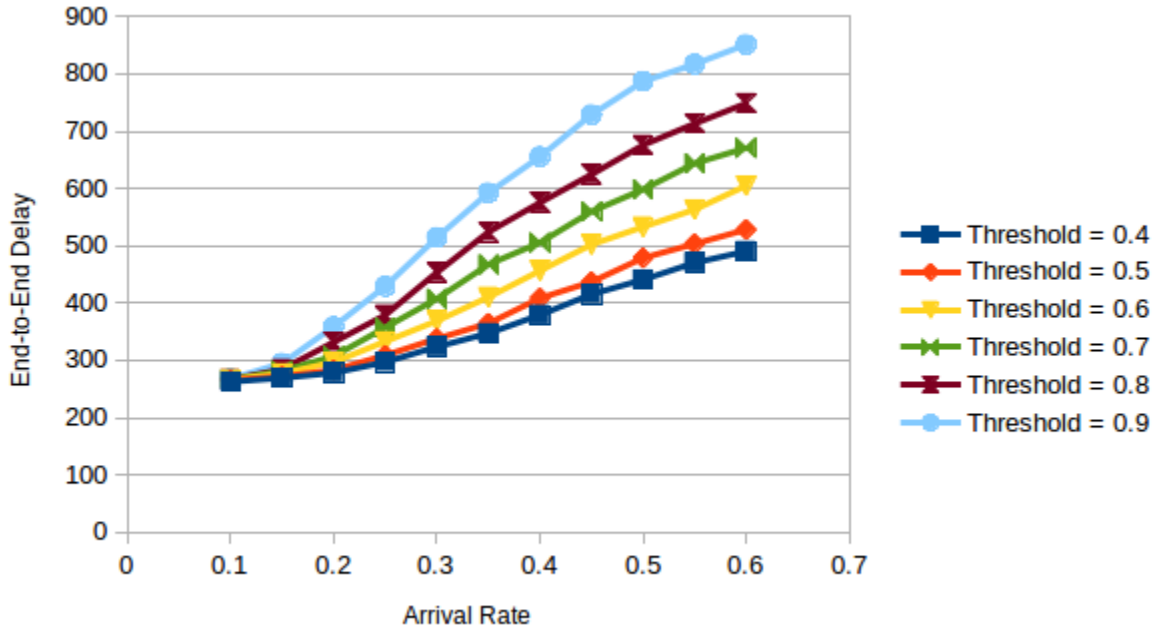


Figure 6.11: Threshold comparison of end-to-end delay vs. arrival rate for: TSP threshold values $\{0.4, 0.5, 0.6, 0.7, 0.8, 0.9\}$

6.4 Performance Without the Adaptive Transmission Rate Protocol

A similar but more extreme approach to addressing the problems that fading causes is to disable the adaptive transmission protocol for the entire network. We examine the network performance without adaptive transmission to show that the TSP protocol’s selective approach is a better solution to the problem. In the following section all links have the same rate and can only transmit one packet per slot.

In Figure 6.12 it is clear that adaptive transmission is important to the performance of the network. Figure 6.1 shows that when there is no fading and the adaptive transmission protocol is enabled the system is able to achieve $\Gamma \approx 0.55$ packets per slot. However, when

the adaptive transmission protocol is disabled, Γ with no fading present decreases to about 0.35 packets per slot, as shown in Figure 6.12. This significant decrease in performance when no fading is present makes disabling the adaptive transmission protocol an undesirable solution.

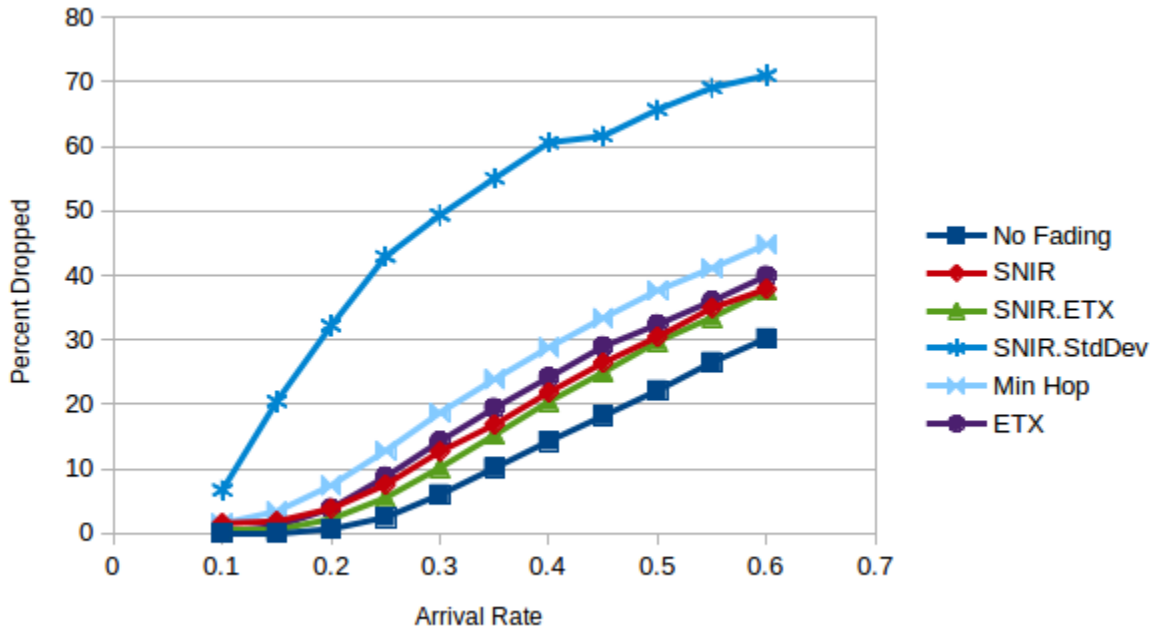


Figure 6.12: Percent Dropped vs. Arrival Rate without adaptive transmission for: No Fading, SNIR, SNIR.ETX, SNIR.StdDev, Min Hop, and ETX

With the adaptive transmission protocol disabled the SNIR routing metric is able to respond reasonably well to the effects of fading, given the performance shown by the system with no fading. This metric shows improvement over the SNIR.StdDev, min hop, and ETX routing metrics. The SNIR.ETX routing metric shows slightly fewer packets being dropped in the presence of fading compared to the SNIR routing metric, but the improvements are not nearly as drastic as when the adaptive transmission protocol is enabled. This suggests that, if the adaptive transmission protocol is disabled, there is not as much need for a

change from the SNIR routing metric.

It is clearly shown in Figure 6.12 that the SNIR.StdDev metric performs very poorly when the adaptive transmission protocol is disabled. The reason for this can be seen by referring back to Figure 6.7. It is shown that the SNIR.StdDev metric does a decent job of reducing the number of packets dropped due to re-transmission attempts, but reducing re-transmission drops is also the primary benefit of disabling the adaptive transmission protocol. Likewise, the SNIR.StdDev metric results in a large number of packets dropped due to buffer overflows, and this issue is further exacerbated by disabling the adaptive transmission protocol. The same considerations that make the SNIR.StdDev metric a poor candidate to be used in conjunction with the TSP protocol also result in poor performance when the adaptive transmission protocol is disabled.

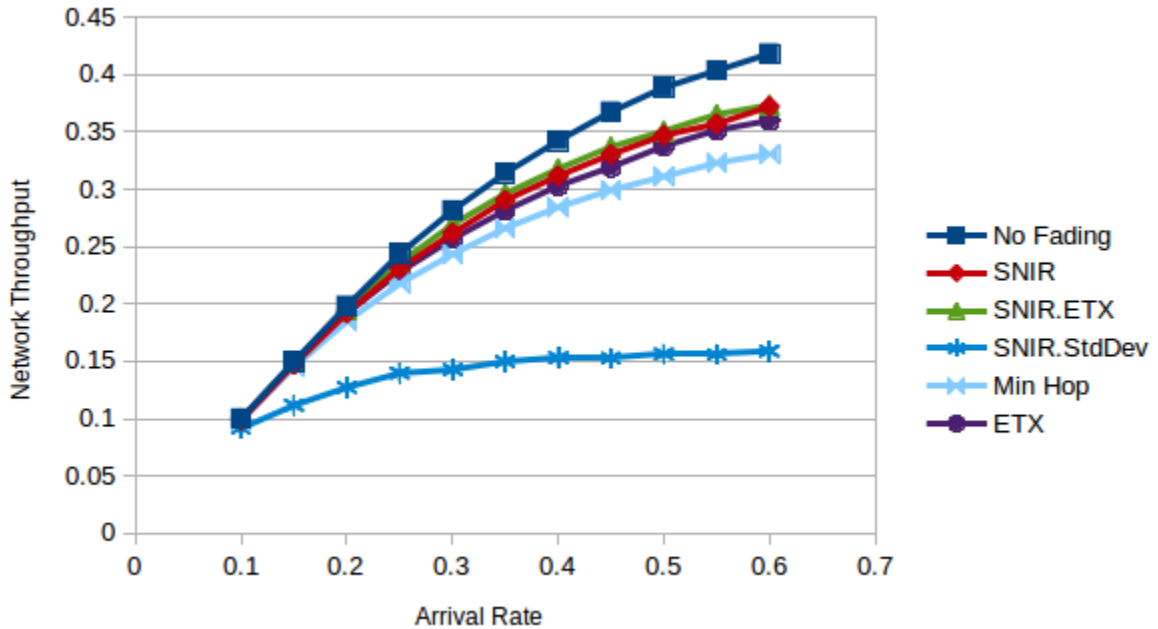


Figure 6.13: Network Throughput vs. Arrival Rate without adaptive transmission for: No Fading, SNIR, SNIR.ETX, SNIR.StdDev, Min Hop, and ETX

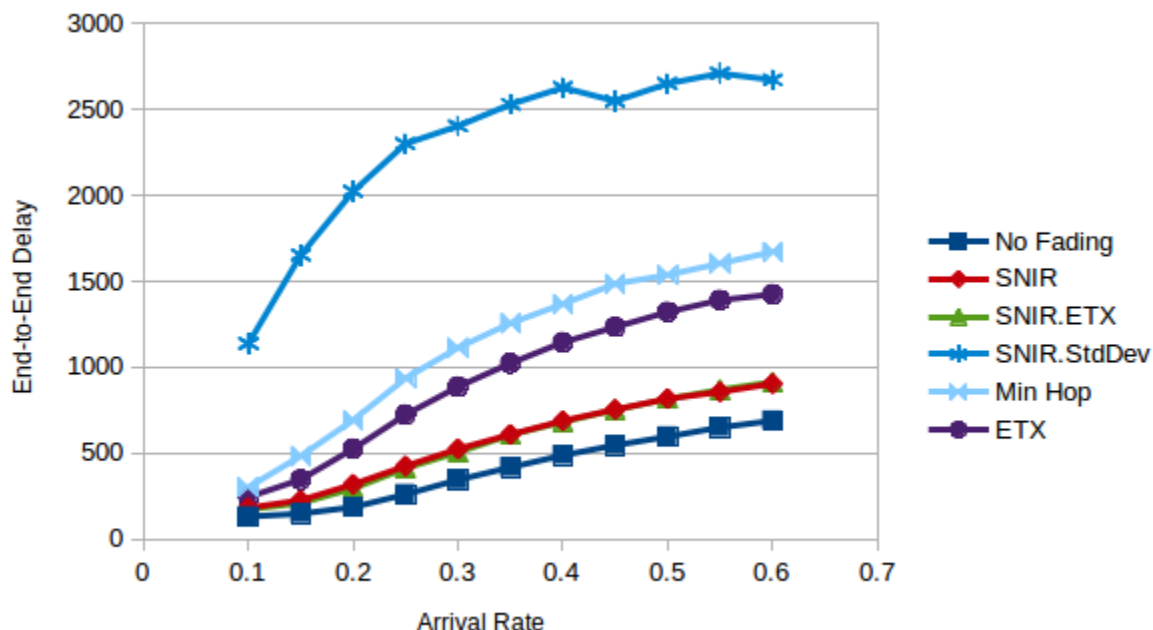


Figure 6.14: End-to-End Delay vs. Arrival Rate without adaptive transmission for: No Fading, SNIR, SNIR.ETX, SNIR.StdDev, Min Hop, and ETX

Figures 6.13 and 6.14 show how the network performs in terms of throughput and delay, respectively. Both of these measures show similar trends compared to the results presented for the percent dropped measure. The SNIR.StdDev metric performs very poorly without the adaptive transmission protocol, and the highest achievable throughput is approximately 0.15 packets/slot, which is much less than that achieved with the other routing metrics. For the other routing metrics, disabling the adaptive transmission protocol still requires that a routing metric be selected that can appropriately respond to the link quality, such as choosing the SNIR metric over the min hop metric. However, the variability in link performance created by the fading environment does not significantly change the routing strategy when an adaptive transmission protocol is not employed. Even so, the best routing metric that we examined does not achieve the network performance that is possible if

the adaptive transmission protocol is enabled and our TSP protocol is used to respond to fading.

6.5 System Performance in Different Network Environments

It is important to verify that the TSP protocol shows performance improvements for different network densities and levels of fading. In this section we show how our TSP protocol performs in more densely connected networks. Sparser networks are not examined, as a high percentage of networks are disconnected at densities lower than those utilized for the investigations reported in the previous sections. We also evaluate the TSP protocol for a range of fading levels. We show that while the network performance is sensitive to the level of fading, the performance of our TSP protocol and the choice of the routing metric is robust among these different fading environments.

Different Network Densities

In the previous sections, the network performance is examined for networks with a relatively low density (the field length is 2000m for all of the previous investigations). In this section the network density is changed to show how density impacts the system performance. Table 6.3 shows how the changes to the field length impact the network density in terms of the network diameter and the average number of one-hop neighbors.

Field Length	Network Diameter	Average Number of Neighbors
2000m	17.23 hops	15.81
1500m	12.18 hops	25.81
1250m	9.99 hops	35.80

Table 6.3: Network density measures based on field length

Figure 6.15 shows how the network performs when the density is increased. Increasing the density does not result in any noticeable change in the percentage of packets

dropped when no fading is present, but in the presence of fading a denser network results in a smaller percentage of packets dropped. For example the SNIR routing metric experiences a packet drop rate of approximately 7% at lower arrival rates, for a field length of 1250m and the TSP protocol disabled. This result is compared to the approximately 20% of packets dropped when the field length is 2000m, as shown in Figure 6.1. Similar relative reductions in the packet drop rate are seen for all the other protocol combinations compared to networks with a lower density.

The system is better able to withstand the effects of fading in denser networks, because Lyui's algorithm reduces the MAI present as the density increases. Figure 6.16 shows that the number of re-transmission drops for SNIR and SNIR.ETX significantly decreases as the network becomes more dense. In these denser networks the 2-hop neighborhoods are much larger. This means that there are more unique color numbers in use, which results in fewer nodes transmitting in the same slot. The nodes that are transmitting experience a better network environment on average, due to the reduced MAI, and on average more fading is required for a transmission to fail.

While a denser network environment reduces MAI and lowers the drop rate, packets experience greater end-to-end delay as shown in Figure 6.17. In denser networks, the frame lengths are longer and fewer nodes can transmit in the same slot, hence packets spend more time in queues and the delay increases. However, it is also shown that the TSP protocol has less of an effect on end-to-end delay as network density increases. The reduced MAI means on average links have higher transmission success probabilities, which results in TSP reducing the transmission rate of fewer links. And a higher average link rate in the network results in less delay.

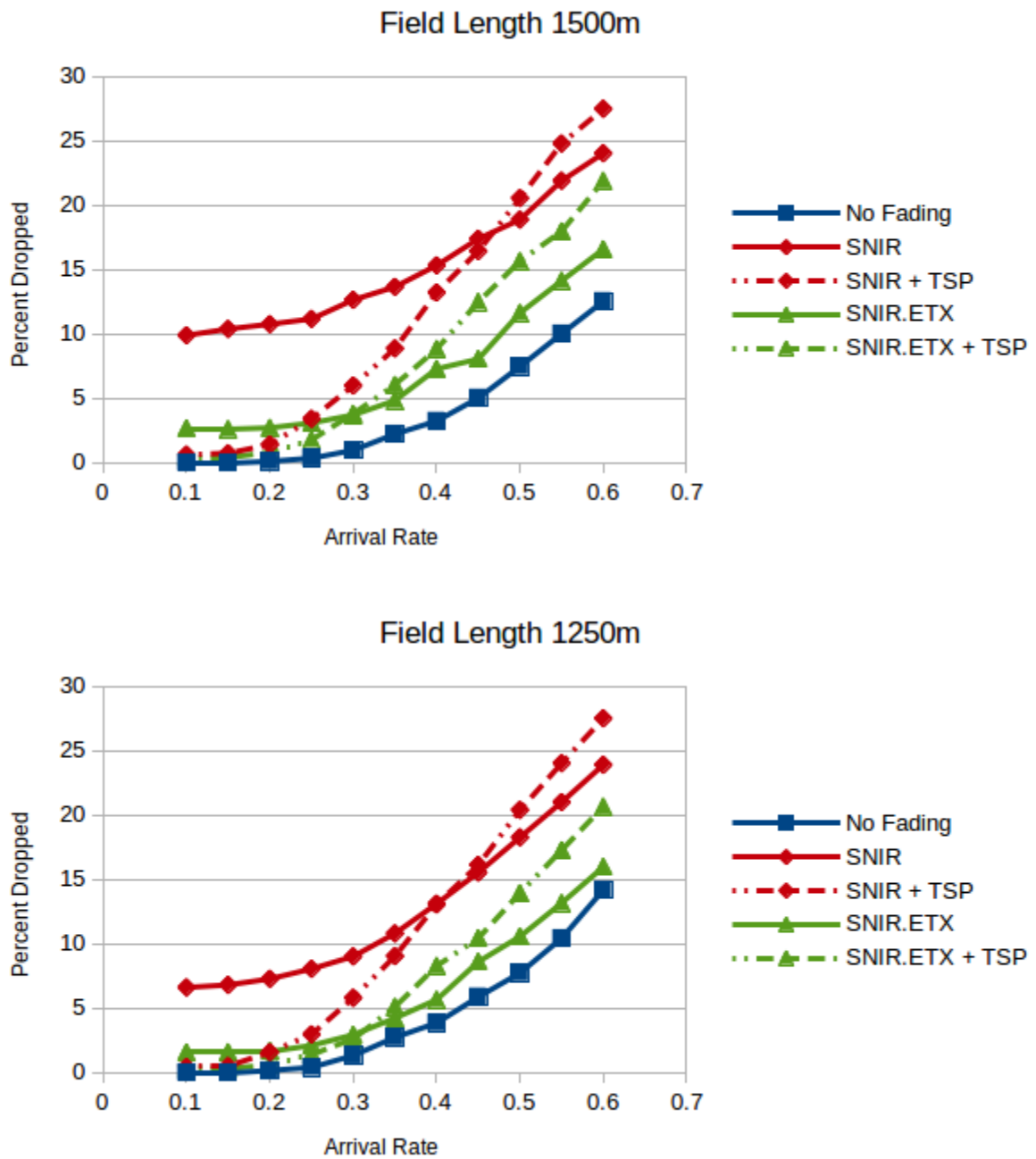


Figure 6.15: Percent Dropped vs. Arrival Rate with field lengths of 1500 and 1250 m for: No Fading, SNIR, SNIR + TSP, SNIR.ETX, and SNIR.ETX + TSP

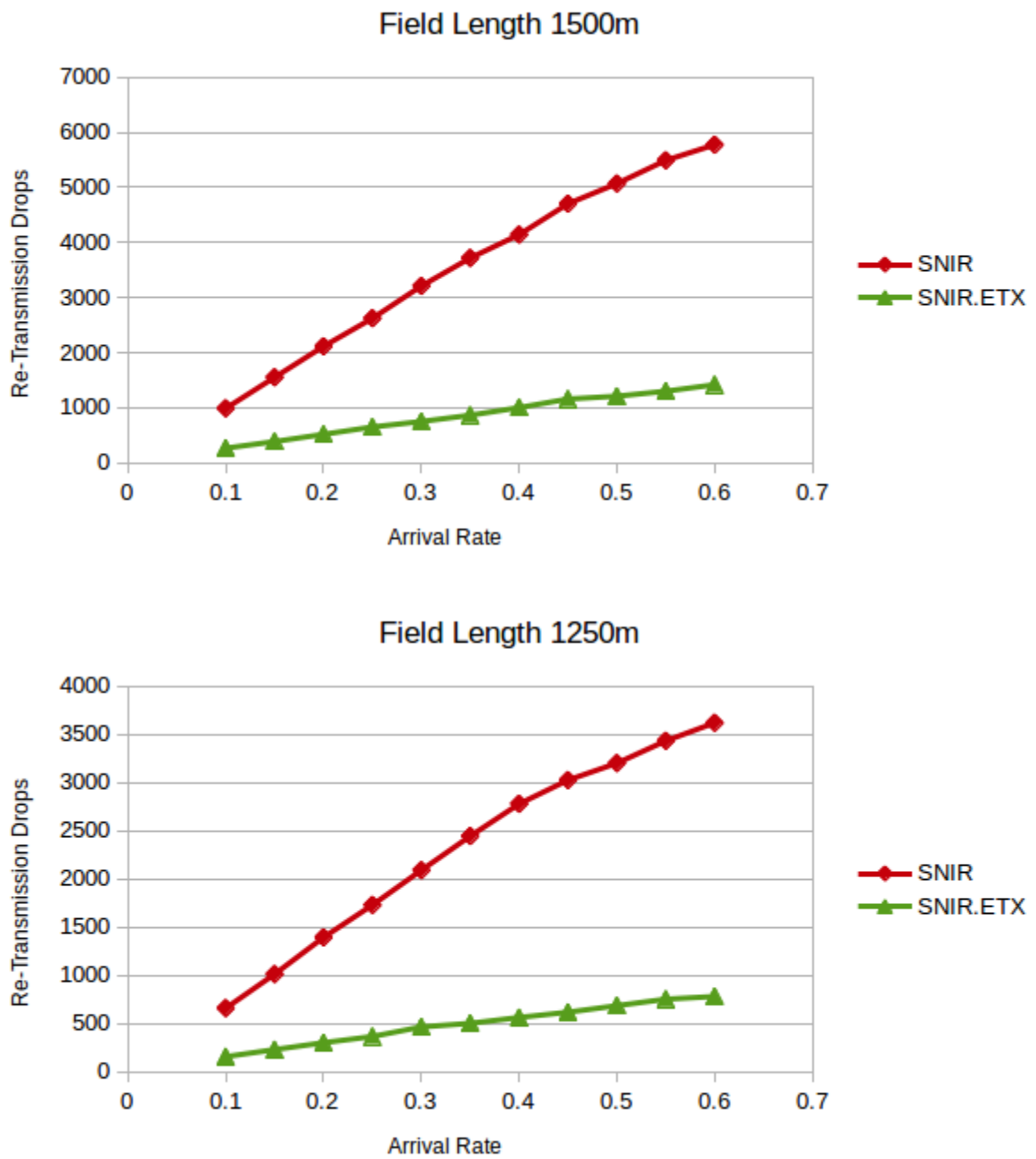


Figure 6.16: Re-Transmission Drops vs. Arrival Rate with field lengths of 1500m and 1250m for: SNIR and SNIR.ETX

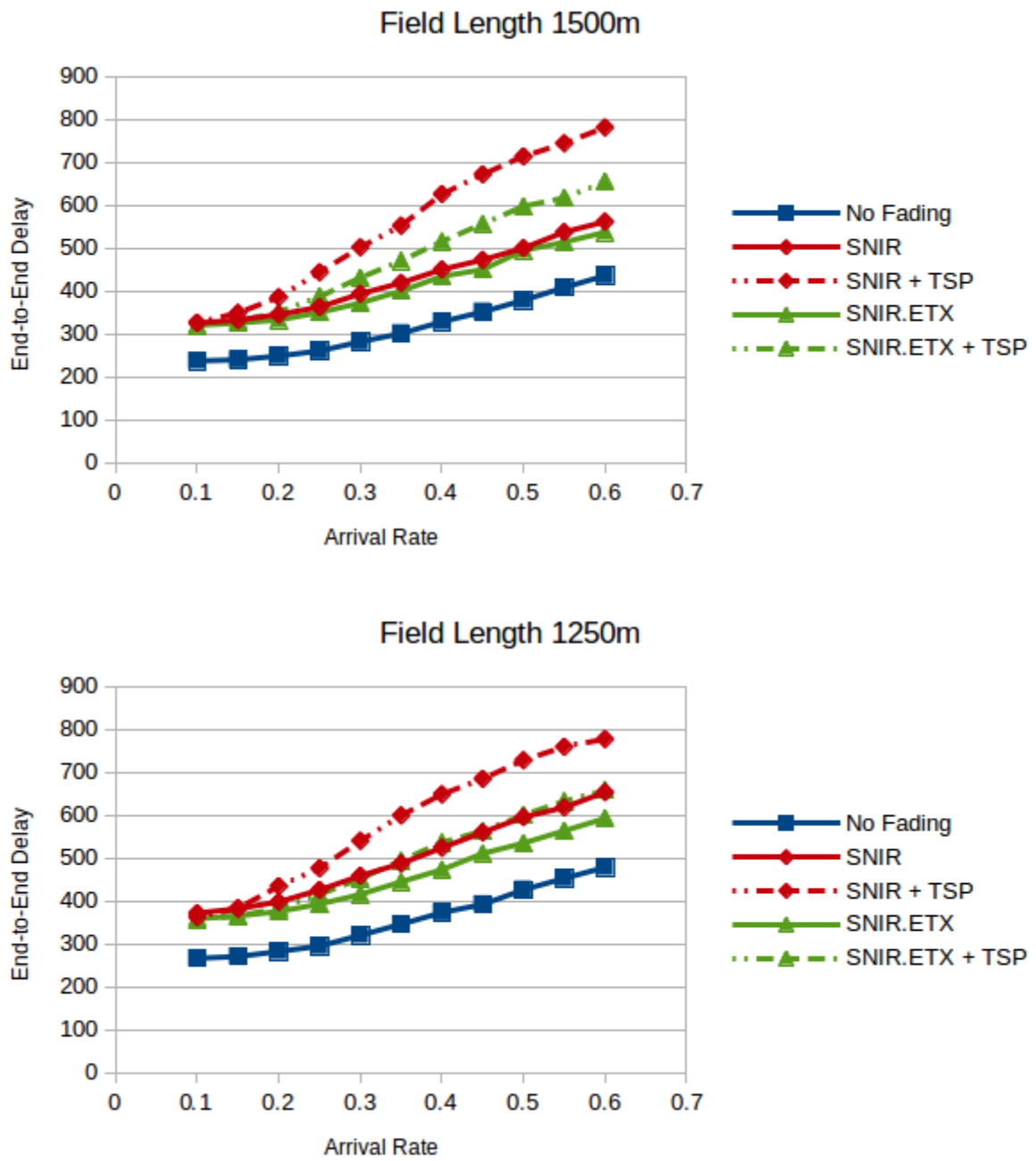


Figure 6.17: End-to-End Delay vs. Arrival rate with field lengths of 1500m and 1250m for: No Fading, SNIR, SNIR + TSP, SNIR.ETX, and SNIR.ETX + TSP

A denser network results in the routing metric having a greater impact than the TSP protocol on the system performance. Take for example, the SNIR.ETX routing metric. If the field length is 1250m (the densest networks we considered), the SNIR.ETX metric is able to respond to the fading environment reasonably well. The TSP protocol provides a small improvement at lower arrival rates, but at higher rates the TSP protocol results in slightly worse performance. This is because fewer of the links with high fading levels are employed and the SNIR.ETX routing metric is able to select among a larger number of higher quality links. In fact, aggressively reducing the data rate with the TSP protocol is unnecessarily limiting the rate packets are forwarded. This suggests that additional investigations into tuning the behavior of the TSP protocol (such as setting the TSP parameter) are needed. This is a topic for future work.

Different Fading Levels

In the remainder of this section the field length is again set to 2000m, but fading levels higher and lower than the 0-5dB used in previous investigations are explored. System performance with higher levels of fading is shown in figure 6.18. The impact of the TSP protocol increases as the level of fading does. The performance decreases in all cases when fading increases, but the decrease in performance is more drastic for systems not using the TSP protocol. When the fading is increased to 0-7dB changing the routing metric to SNIR.ETX does not yield a γ that has fewer than 10% of packets dropped. Enabling TSP still reduces the percentage of packets dropped to below 10% for small γ , but the increased fading results in a reduced Γ . Increasing the fading from 0-5dB to 0-7dB decreases Γ of SNIR.ETX + TSP by about 0.05 packets/slot. Γ is further reduced by the same amount when the fading is increased to 0-10dB.

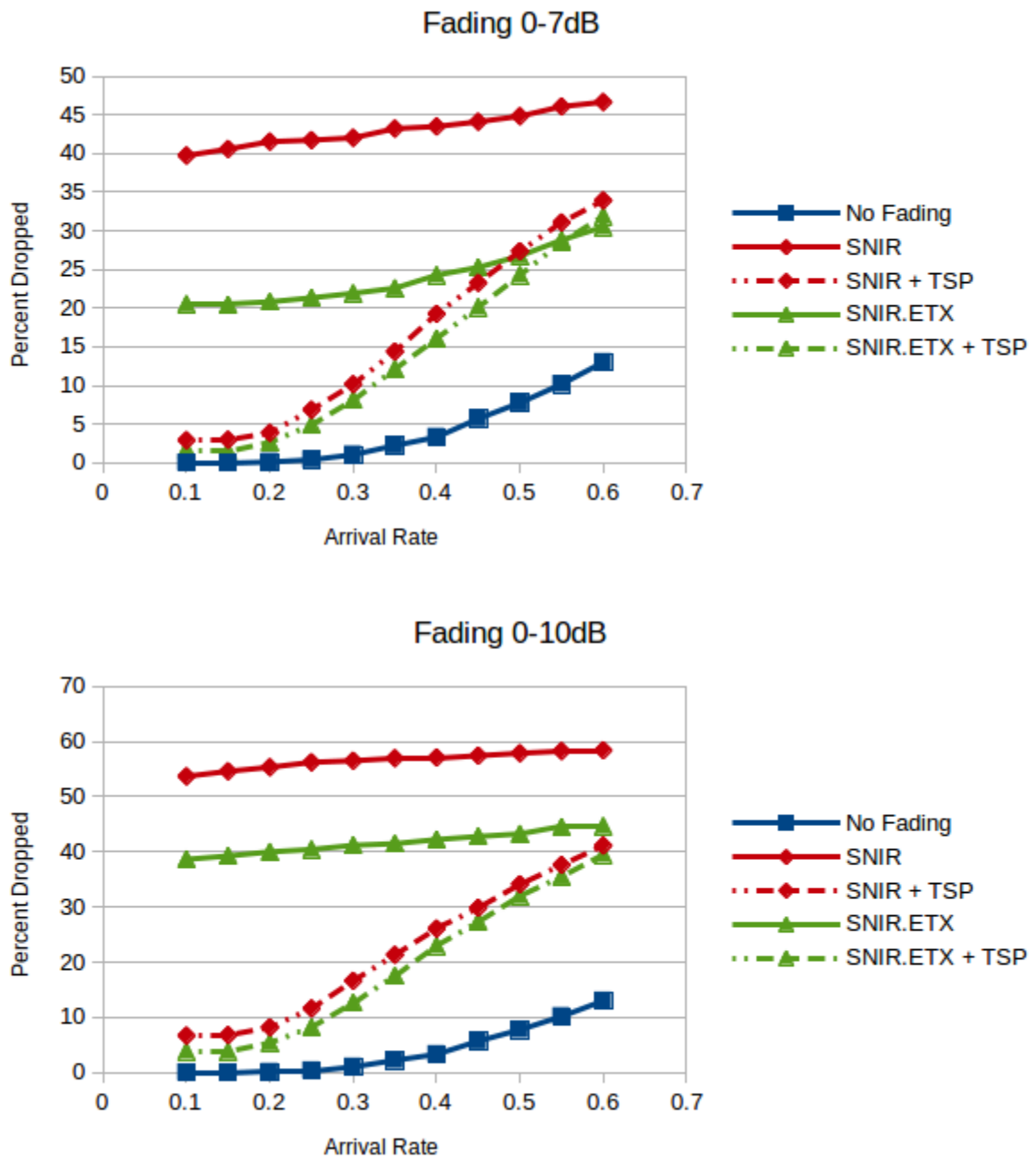


Figure 6.18: Percent Dropped vs. Arrival Rate with 0-7dB and 0-10dB of fading for: No Fading, SNIR, SNIR + TSP, SNIR.ETX, and SNIR.ETX + TSP

Figure 6.19 shows that there is less need for the TSP protocol at lower levels of fading. The TSP protocol still provides better performance for smaller γ , but results in a reduction in Γ at lower fading levels. While the reduction in performance is small, this shows that at lower fading levels more emphasis needs to be put on balancing the number of re-transmission drops and buffer overflows. More information about the links could be used to improve the performance of the TSP protocol. A future analysis of the system bottle necks may suggest new routing metrics that work better with the TSP protocol.

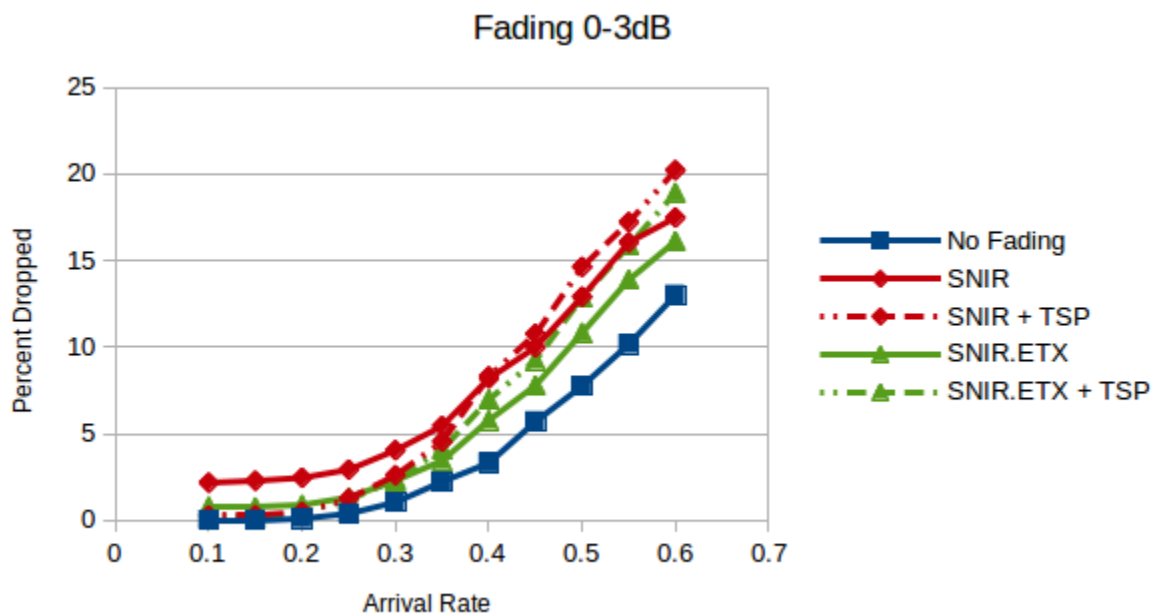


Figure 6.19: Percent Dropped vs. Arrival Rate with 0-3dB of fading for: No Fading, SNIR, SNIR + TSP, SNIR.ETX, and SNIR.ETX + TSP

Chapter 7

Conclusions

This work provides a method for controlling link rate adaption to minimize the impacts of a fading environment. We have shown that fading causes a significant decrease in network performance when the problem is not addressed. We proposed the TSP link rate control protocol as a solution for handling fading, and we have shown that the TSP protocol significantly improves network performance in the presence of fading by using transmission success probabilities as a measure of link variability to selectively reduce the transmission rates of links most impacted by fading. We have shown that the TSP protocol's selective approach to link rate control is a better solution than disabling the adaptive transmission protocol network wide. The benefits of the TSP protocol are more noticeable at higher levels of fading. But when there is less fading the TSP protocol results in slightly worse network performance.

It is shown that the routing metric used in conjunction with the TSP protocol can significantly change the system performance, and that a routing metric should not be selected based solely on the performance of the routing metric without the TSP protocol. We proposed two different modifications to the base SNIR routing metric. First, the SNIR.ETX metric is shown to perform well in a wide range of scenarios by including a measure of the link success rate in the metric. Second, we proposed the SNIR.StdDev metric, which uses an estimated measure of the standard deviation of the SNIR to avoid highly variable links. The

SNIR.ETX routing metric is an improvement over the SNIR routing metric when fading is present, and is further improved by the addition of the TSP protocol. However, while the SNIR.StdDev metric performs well without the TSP protocol, when the TSP protocol is used in conjunction with this routing metric performance degrades quickly. We have shown through the measures of packets dropped due to buffer overflows versus re-transmissions, that the best approach may be to use the TSP protocol in conjunction with a routing metric that focuses on avoiding bottlenecks in the network.

Moving forward the TSP protocol needs to be tested in a mobile network. The protocol is simple, and the exchange of information should not be prohibitive in a mobile environment. However, when nodes are mobile there may not be enough time to gather sufficient transmission success probability measures in order to make decisions. A mechanism for recovering link rates after being reduced by the TSP protocol is also of significant interest. In a mobile environment the level of fading experienced between two given nodes is likely to change, and links with highly variable performance could become more reliable over time.

In this investigation network control packets were assumed to be instantaneous and have a perfect success rate. In the future it should be shown what happens when the fading environment causes control packets to be lost. Additionally the loss acknowledgment packets may impair the performance of the TSP protocol. Methods for securing control packets against loss due to fading should be investigated. These methods will likely look different as control packets are often transmitted at a slower and more reliable transmission rate.

References

- [1] A. Kush and S. Taneja, "A Survey of Routing Protocols in Mobile Ad Hoc Networks," *International Journal of Innovation, Management and Technology*, vol. 1, no. December, pp. 30–38, 2010.
- [2] G. V. Kumar, Y. V. Reddy, and D. M. Nagendra, "Current research work on routing protocols for MANET: a literature survey," *international Journal on computer Science and Engineering*, vol. 2, no. 03, pp. 706–713, 2010.
- [3] M. B. Pursley, H. B. Russell, and J. S. Wycarski, "Energy-efficient routing in frequency-hop networks with adaptive transmission," *Proceedings - IEEE Military Communications Conference MILCOM*, vol. 2, pp. 1409–1413, 1999.
- [4] B. Wolf, *CROSS-LAYER SCHEDULING PROTOCOLS FOR MOBILE AD HOC NETWORKS USING ADAPTIVE DIRECT-SEQUENCE SPREAD-*. PhD thesis, Clemson University, 2010.
- [5] D. S. J. De Couto, D. Aguayo, J. Bicket, and R. Morris, "A High-throughput Path Metric for Multi-hop Wireless Routing," *Wirel. Netw.*, vol. 11, pp. 419–434, jul 2005.
- [6] S. Kumar, V. S. Raghavan, and J. Deng, "Medium Access Control protocols for ad hoc wireless networks: A survey," *Ad Hoc Networks*, vol. 4, no. 3, pp. 326–358, 2006.
- [7] C. D. Young, "USAP: a unifying dynamic distributed multichannel TDMA slot assignment protocol," in *Military Communications Conference, 1996. MILCOM '96, Conference Proceedings, IEEE*, vol. 1, pp. 235–239 vol.1, oct 1996.
- [8] C. D. Young, "USAP multiple access: dynamic resource allocation for mobile multihop multichannel wireless networking," in *MILCOM 1999. IEEE Military Communications Conference Proceedings (Cat. No.99CH36341)*, vol. 1, pp. 271–275 vol.1, 1999.
- [9] W.-P. Luyi, *Design of a new operational structure for mobile radio networks*. PhD thesis, Clemson University, 1991.
- [10] P. K. Appani, *Collision-free scheduling for ad hoc networks*. mastersthesis, Clemson University, 2003.
- [11] D. J. Vergados, N. Amelina, Y. Jiang, K. Kralevska, and O. Granichin, "Local Voting: Optimal Distributed Node Scheduling Algorithm for Multihop Wireless Networks," *arXiv preprint arXiv:1703.00731*, 2017.

- [12] V. B. Subrahmanya and H. B. Russell, "Recovering the reserved transmission time slots in an ad hoc network with scheduled channel access," in *MILCOM 2016 - 2016 IEEE Military Communications Conference*, pp. 67–72, nov 2016.
- [13] J. H. Gass Jr., M. B. Pursley, H. B. Russell, and J. S. Wycarski, "An Adaptive-transmission Protocol for Frequency-hop Wireless Communication Networks," *Wirel. Netw.*, vol. 7, pp. 487–495, sep 2001.
- [14] J. P. Pavon and S. Choi, "Link adaptation strategy for IEEE 802.11 WLAN via received signal strength measurement," in *Communications, 2003. ICC '03. IEEE International Conference on*, vol. 2, pp. 1108–1113 vol.2, may 2003.
- [15] M. Lacage, M. H. Manshaei, and T. Turletti, "IEEE 802.11 Rate Adaptation: A Practical Approach," in *Proceedings of the 7th ACM International Symposium on Modeling, Analysis and Simulation of Wireless and Mobile Systems, MSWiM '04*, (New York, NY, USA), pp. 126–134, ACM, 2004.
- [16] T. Rappaport, *Wireless Communications: Principles and Practice*. Upper Saddle River, NJ, USA: Prentice Hall PTR, 2nd ed., 2001.
- [17] M. A. Juang and M. B. Pursley, "New results on finite-state Markov models for Nakagami fading channels," in *2011 - MILCOM 2011 Military Communications Conference*, pp. 453–458, nov 2011.
- [18] M. A. Juang and M. B. Pursley, "Finite-State Markov Chain Models for the Intensity of Nakagami Fading," *International Journal of Wireless Information Networks*, vol. 20, no. 2, pp. 95–102, 2013.
- [19] A. I. Sulyman, A. T. Nassar, M. K. Samimi, G. R. Maccartney, T. S. Rappaport, and A. Alsanie, "Radio propagation path loss models for 5G cellular networks in the 28 GHZ and 38 GHZ millimeter-wave bands," *IEEE Communications Magazine*, vol. 52, pp. 78–86, sep 2014.
- [20] V. Bhaskar, "Finite-state Markov Model for Lognormal, Chi-square (Central), Chi-square (Non-central), and K-distributions," *International Journal of Wireless Information Networks*, vol. 14, no. 4, pp. 237–250, 2007.
- [21] M. D. Renzo, F. Graziosi, and F. Santucci, "A comprehensive framework for performance analysis of cooperative multi-hop wireless systems over log-normal fading channels," *IEEE Transactions on Communications*, vol. 58, pp. 531–544, feb 2010.
- [22] A. J. Goldsmith and S. B. Wicker, "Design challenges for energy-constrained ad hoc wireless networks," *IEEE Wireless Communications*, vol. 9, pp. 8–27, aug 2002.